Supplementary information

A Neutral $\sigma^0\pi^2$ Carbene Enabling Hydrogen Activation via a σ-Face Pathway

Fei Fan, Haoxiang Nong, Miaomiao Zhou, Liu Leo Liu*
Department of Chemistry and Research Center for Chemical Biology and Omics Analysis, College of Science, Southern University of Science and Technology, Shenzhen 518055, China

Table of Contents

I. Materials and Methods S3
II. Experimental Details and Characterization Data S4
III. NMR Spectra S8
IV. HRMS Spectra S18
V. X-ray Crystallographic Data S20
VI. Photophysical Data S23
VII. Kinetic Experiments S25
7.1 Time-course kinetics for D_2. ..... S25
7.2 KIE determination from the initial-rate regime. S27
VIII. Computational Details S29
8.1 Geometry optimization and singlet–triplet energy gap of **2**. S30
8.2 TDDFT calculations of **2** S31
8.3 NMR calculations S32
8.4 Regarding the observed asynchronicity S36
8.5 IBO calculations for **2**. S39
8.6 FMOs calculations for cationic $\sigma^0\pi^2$ carbene **A**. S40
8.7 Gibbs free energy profiles for H_2 activation by **2** and **CAAC** (kcal/mol). S41
8.8 Heavy-atom root-mean-square deviation (RMSD) of **2** and **CAAC** S42
8.9 Activation strain model (ASM) analysis of **2** and **CAAC** S43
8.10 NLMOs of **TS1** and **TS2** S44
8.11 2D deformation density and ELF maps. S45
IX. References S65

I. Materials and Methods

All manipulations were conducted within a nitrogen-filled glovebox or under a dry nitrogen atmosphere, employing standard Schlenk techniques, unless otherwise specified. *n*-hexane, *n*-pentane, and tetrahydrofuran (THF) and dichloromethane (DCM) were subjected to distillation over sodium/potassium, $LiAlH_4$ or CaH_2 and subsequently stored over activated molecular sieves in the glove box. Commercial reagents were purchased from Energy Chemical, J&K, or TCI Chemical Co. and used as received. α-(bisphosphino)diazomethane **1**(*1*) and Rh(cod)(allyl) (cod = 1,5-cyclooctadiene)(*2*) were prepared according to the procedure described in the literature. Mes represents mesityl (mesityl = 1,3,5-$Me_3C_6H_2$). Deuterated solvents, such as C_6D_6 and THF-d_8, were degassed by employing three freeze–pump–thaw cycles and stored over activated molecular sieves in the glovebox. NMR spectra were acquired at 298 K on a Bruker Avance 400 (^{1}H: 400 MHz, ^{31}P: 162 MHz, ^{13}C: 101 MHz) or 600 (^{1}H: 600 MHz, ^{31}P: 243 MHz, ^{13}C: 151 MHz) NMR spectrometer. The provided data is presented as follows: chemical shift, multiplicity (s = singlet, d = doublet, t = triplet, q = quartet, dt = doublet of triplets, td = triplet of doublets, br = broad, m = multiplet and/or multiple resonances), coupling constant in hertz (Hz), integration and attribution.

High-resolution mass spectrometry (HRMS) was conducted using a Thermo Fisher Scientific Q-Exactive MS System with electrospray ionization (ESI) method. Infrared spectra were recorded on a FT-IR spectrometer (Bruker ALPHA II) using a DLaTGS detector. UV-Vis absorption spectra were recorded on Lambda 365 spectrophotometer (PerkinElmer) at room temperature.

Crystal data were collected on a Bruker D8 VENTURE diffractometer equipped with either an Excillum METALJET microfocus X-ray source (Ga-Kα, λ = 1.34139 Å) or a Mo-Kα radiation source (λ = 0.71073 Å). Data reduction, scaling and absorption corrections were performed using SAINT (Bruker, V8.38A, 2013). The structures were solved with the XT structure solution program using the Intrinsic Phasing solution method and by using Olex2 as the graphical interface. The frames were integrated with the Bruker SAINT software package using a narrow-frame algorithm. Data was corrected for absorption effects using the empirical multi-scan method (SADABS). The model was refined with the ShelXL program using Least Squares minimization. All non-hydrogen atoms were refined anisotropically. Hydrogen atoms were included in structure factor calculations. All hydrogen atoms were assigned to idealized geometric positions.

To gain deeper insight into the electronic structure, we carried out an experimental charge density analysis based on the X-ray diffraction data using the *MoPro* program. Unlike to the conventional spherical atomic structural parameters refined in routine X-ray diffraction analyses, this approach characterizes the aspherical nature of atomic electron density by introducing the Hansen-Coppens multipolar formalism for individual atoms. Multipolar coefficients were refined up to the dipolar level for hydrogen atoms, the octopolar level for carbon and nitrogen atoms, and the hexadecapolar level for rhodium and phosphorus atoms. The scaling factor was refined sequentially, along with full automatic electron density refinement under specific constraints: multipole symmetry, identical valence and multipole populations for equivalent atoms, and uniform contraction/expansion coefficients (κ values) for equivalent atoms. Finally, the 2D deformation electron density was calculated and visualized using *MoProViewer*.

II. Experimental Details and Characterization Data

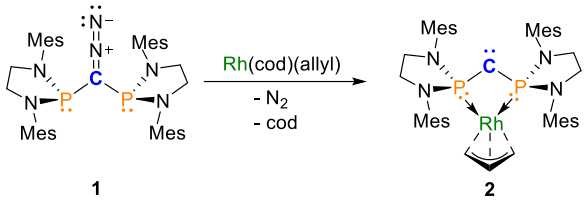

Fig. S1. Synthesis of **2**.

A solution of Rh(cod)(allyl) (17.6 mg, 0.07 mmol) in DCM (1.0 mL) was slowly added to a DCM solution of compound **1** (50.0 mg, 0.07 mmol) (2.0 mL) at -30 °C. After stirring for 0.5 hour, all volatile were evaporated under vacuum, the resulting brown solid was extracted with *n*-hexane (6 mL). Concentration of the *n*-hexane solution yielded compound **2** as an orange-yellow solid (49 mg, 0.05 mmol) in 85% yield. Single crystals (orange-yellow) suitable for X-ray diffraction analysis were obtained through the slow evaporation of a concentrated benzene solution at room temperature.

^{1}H NMR (600 MHz, THF-d_8) δ (ppm) 6.51 (d, J = 6.0 Hz, 8H, ^{Mes}Ar-*H*), 4.36–4.28 (m, 1H, ^{allyl}C*H*), 3.50–3.47 (m, 6H, CH_2 and ^{allyl}CH_2), 3.42–3.38 (m, 4H, CH_2), 2.21 (s, 12 H, ^{Mes}CH_3), 2.15 (s, 12 H, ^{Mes}CH_3), 2.07 (s, 12 H, ^{Mes}CH_3), 1.86–1.83 (m, 2H, ^{allyl}CH_2).

^{13}C{^{1}H} NMR (151 MHz, THF-d_8) δ (ppm) 139.6, 138.9, 137.5 (d, J = 3.0 Hz), 137.48 (d, J = 3.0 Hz), 135.7, 129.8, 129.2, 100.0–99.9 (m, ^{allyl}*C*H), 50.2–50.0 (m, ^{allyl}*C*H$_2$), 48.0 (d, J = 4.5 Hz, *C*H$_2$), 47.98 (d, J = 4.5 Hz, *C*H$_2$), 21.5, 19.4, 19.3, -22.7 (d, $^{2}J_{Rh-C}$ = 10.6 Hz, P*C*P).

^{31}P NMR (243 MHz, THF-d_8) δ (ppm) 88.3 (d, $^{1}J_{Rh-P}$ = 194.4 Hz).

HRMS [M+H]$^{+}$ $C_{44}H_{58}N_4P_2Rh^{+}$ calc. 807.3186 *m/z*, found 807.3183 *m/z*.

IR (ATR, neat): ν = 3059, 2908, 2846, 1608, 1479, 1247, 930 cm^{-1}

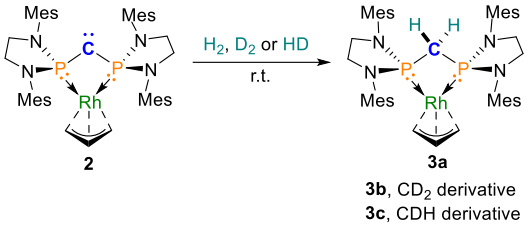

Fig. S2. Synthesis of **3a**, **3b** and **3c**.

A solution of **2** (50.0 mg, 0.06 mmol) in benzene (2.0 mL) was degassed by freeze-pump-thaw cycles 3~5 times, and exposed to 1 atm of H_2 at 10 ºC. The solution was then gradually warmed to room temperature and stirred for another 24 hours, resulting in a color change to brown. All volatiles were removed under vacuum, affording a deep brown solid. The mixture was subsequently extracted with *n*-hexane (3 x 2 mL) and filtered through a pad of celite. Slow evaporation of the concentrated *n*-hexane solution at room temperature afforded orange-yellow crystals **3a**. Yield: 32 mg (0.04 mmol, 67%). Single crystals (orange-yellow) suitable for X-ray diffraction analysis were obtained through the slow evaporation of a concentrated *n*-hexane solution at room temperature.

^{1}H NMR (400 MHz, THF-d_8) δ (ppm) 6.69 (br, 2H, ^{Mes}Ar-*H*), 6.66–6.63 (m, 6H, ^{Mes}Ar-*H*), 4.18 (td, *J* = 8.8 Hz, 1H, PC*H*$_2$P), 3.98–3.87 (m, 2H, ^{allyl}C*H* and PC*H*$_2$P), 3.43–3.34 (m, 4H, C*H*$_2$), 3.32–3.26 (m, 4H, C*H*$_2$), 3.11 (dd, *J* = 7.2, 3.2 Hz, 2H, ^{allyl}C*H*$_2$), 2.39 (s, 6H, ^{Mes}C*H*$_3$), 2.37 (s, 6H, ^{Mes}C*H*$_3$), 2.26 (s, 6H, ^{Mes}C*H*$_3$), 2.23 (s, 6H, ^{Mes}C*H*$_3$), 1.98 (s, 6H, ^{Mes}C*H*$_3$), 1.89 (s, 6H, ^{Mes}C*H*$_3$), 1.23 (dd, *J* = 13.6, 8.0 Hz, 2H, ^{allyl}C*H*$_2$).

^{13}C{^{1}H} NMR (151 MHz, THF-d_8) δ (ppm) 140.9 (d, *J* = 9.1 Hz), 140.88, 140.42 (d, *J* = 9.1 Hz), 140.4, 139.6, 139.4, 139.0, 138.6, 135.6, 135.4, 130.1, 130.0, 129.9, 129.6, 114.5 (br, ^{allyl}*C*H), 81.6 (d, $^{2}J_{Rh-C}$ = 15.1 Hz, P*C*H$_2$P), 55.8 (dd, $^{1}J_{Rh-C}$ = 34.7, $^{2}J_{P-C}$ = 6.0 Hz, ^{allyl}*C*H$_2$), 51.3, 51.1, 21.66 (d, *J* = 3.0 Hz), 21.64 (d, *J* = 3.0 Hz), 21.4, 21.3, 21.2, 19.6, 19.5.

^{31}P NMR (162 MHz, THF-d_8) δ (ppm) 71.0 (d, $^{1}J_{Rh-P}$ = 251.1 Hz).

HRMS [M-allyl]$^{+}$ $C_{41}H_{54}N_4P_2Rh^{+}$ calc. 767.2873 *m/z*, found 767.2868 *m/z*.

A solution of **2** (40.0 mg, 0.05 mmol) in benzene (2.5 mL) was degassed by freeze-pump-thaw cycles 3~5 times, and exposed to 1 atm of D_2 at 10 °C. The solution was then gradually warmed to room temperature and stirred for another 24 hours, resulting in a color change to brown. All volatiles were removed under vacuum, affording a deep brown solid. The mixture was subsequently extracted with *n*-hexane (3 x 2 mL) and filtered through a pad of celite. Slow evaporation of the concentrated *n*-hexane solution at room temperature afforded orange-yellow crystals **3b**. Yield: 24 mg (0.03 mmol, 60%).

^{1}H NMR (400 MHz, THF-d_8) δ (ppm) 6.69 (br, 2H, ^{Mes}Ar-*H*), 6.66–6.63 (m, 6H, ^{Mes}Ar-*H*), 3.98–3.87 (m, 1H, ^{allyl}C*H*), 3.43–3.36 (m, 4H, CH_2), 3.35–3.24 (m, 4H, CH_2), 3.11 (dd, J = 7.2, 3.2 Hz, 2H, ^{allyl}CH_2), 2.39 (s, 6H, ^{Mes}CH_3), 2.37 (s, 6H, ^{Mes}CH_3), 2.26 (s, 6H, ^{Mes}CH_3), 2.23 (s, 6H, ^{Mes}CH_3), 1.98 (s, 6H, ^{Mes}CH_3), 1.89 (s, 6H, ^{Mes}CH_3), 1.23 (dd, J = 16.0, 8.0 Hz, 2H, ^{allyl}CH_2).

^{13}C{^{1}H} NMR (151 MHz, THF-d_8) δ (ppm) 140.9 (d, J = 9.1 Hz), 140.89, 140.44 (d, J = 7.6 Hz), 140.3, 139.6, 139.4, 139.0, 138.6, 135.6, 135.4, 130.1, 130.0, 129.9, 129.6, 114.5 (br, ^{allyl}*C*H), 81.7–81.0 (m, P*C*D$_2$P), 55.8 (dd, $^1J_{Rh\text{-}C}$ = 34.7, $^2J_{P\text{-}C}$ = 6.0 Hz, ^{allyl}*C*H$_2$), 51.3, 51.1, 21.65 (d, J = 3.0 Hz), 21.63 (d, J = 3.0 Hz), 21.4, 21.3, 21.1, 19.6, 19.5.

^{2}H NMR (92 MHz, THF-d_8) δ (ppm) 4.14 (br, 1D, PCD_2P), 3.90 (br, 1D, PCD_2P).

^{31}P NMR (162 MHz, THF-d_8) δ (ppm) 68.7 (d, $^1J_{Rh\text{-}P}$ = 247.9 Hz).

HRMS [M-allyl]$^+$ $C_{41}H_{52}D_2N_4P_2Rh^+$ calc. 769.2999 *m/z*, found 769.2974 *m/z*.

A solution of **2** (40.0 mg, 0.05 mmol) in benzene (2.5 mL) was degassed by freeze-pump-thaw cycles 3~5 times, and exposed to 1 atm of HD at 10 °C. The solution was then gradually warmed to room temperature and stirred for another 24 hours, resulting in a color change to brown. All volatiles were removed under vacuum, affording a deep brown solid. The mixture was subsequently extracted with *n*-hexane (3 x 2 mL) and filtered through a pad of celite. Slow evaporation of the concentrated *n*-hexane solution at room temperature afforded orange-yellow crystals **3c**. Yield: 25 mg (0.03 mmol, 62%).

^{1}H NMR (600 MHz, THF-d_8) δ (ppm) 6.69 (br, 2H, ^{Mes}Ar-*H*), 6.66–6.63 (m, 6H, ^{Mes}Ar-*H*), 4.20–4.15 (m, 0.47H, PC*H*DP), 3.96–3.89 (m, 1.53H, ^{allyl}C*H* and PC*H*DP), 3.45–3.35 (m, 4H, CH_2), 3.33–3.26 (m, 4H, CH_2), 3.11 (dd, J = 7.2, 2.4 Hz, 2H, ^{allyl}CH_2), 2.39 (s, 6H, ^{Mes}CH_3), 2.37 (s, 6H, ^{Mes}CH_3), 2.26 (s, 6H, ^{Mes}CH_3), 2.23 (s, 6H, ^{Mes}CH_3), 1.98 (s, 6H, ^{Mes}CH_3), 1.89 (s, 6H, ^{Mes}CH_3), 1.23 (dd, J = 13.6, 7.8 Hz, 2H, ^{allyl}CH_2).

^{13}C{^{1}H} NMR (151 MHz, THF-d_8) δ (ppm) 140.9 (d, J = 9.1 Hz), 140.44 (d, J = 9.1 Hz), 140.4, 139.6, 139.4, 139.0, 138.6, 135.6, 135.4, 130.1, 130.0, 129.9, 129.6, 114.5 (br, ^{allyl}*C*H), 81.7–81.2 (m, P*C*HDP), 55.8 (dd, $^{1}J_{Rh-C}$ = 34.7, $^{2}J_{P-C}$ = 6.0 Hz, ^{allyl}*C*H$_2$), 51.3, 51.1, 21.65 (d, J = 3.0 Hz), 21.63 (d, J = 4.5 Hz), 21.4, 21.3, 21.1, 19.6, 19.5.

^{2}H NMR (92 MHz, THF-d_8) δ (ppm) 4.15 (br, 0.47D, PCH*D*P), 3.90 (br, 0.53D, PCH*D*P).

^{31}P NMR (243 MHz, THF-d_8) δ (ppm) 70.3 (d, $^{1}J_{Rh-P}$ = 250.3 Hz).

HRMS [M-allyl]$^{+}$ $C_{41}H_{53}DN_4P_2Rh^{+}$ calc. 768.2936 *m/z*, found 768.2921 *m/z*.

III. NMR Spectra

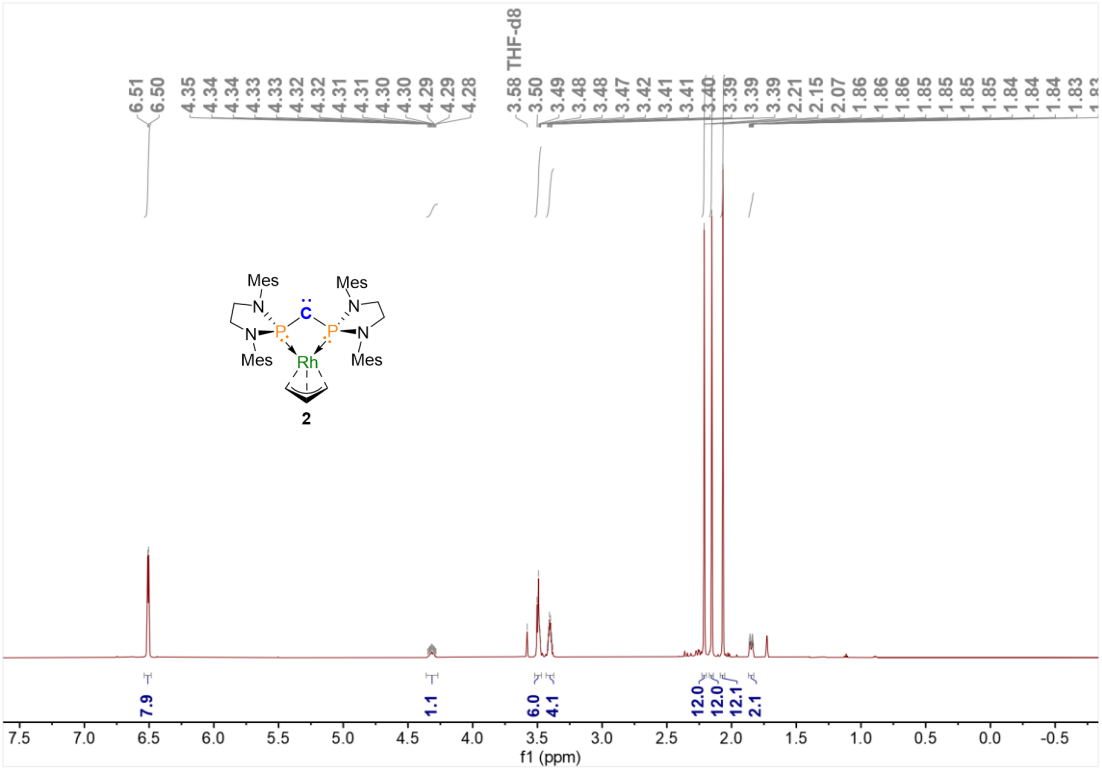

Fig. S3. ^{1}H NMR spectrum of **2** (600 MHz, THF-d_8).

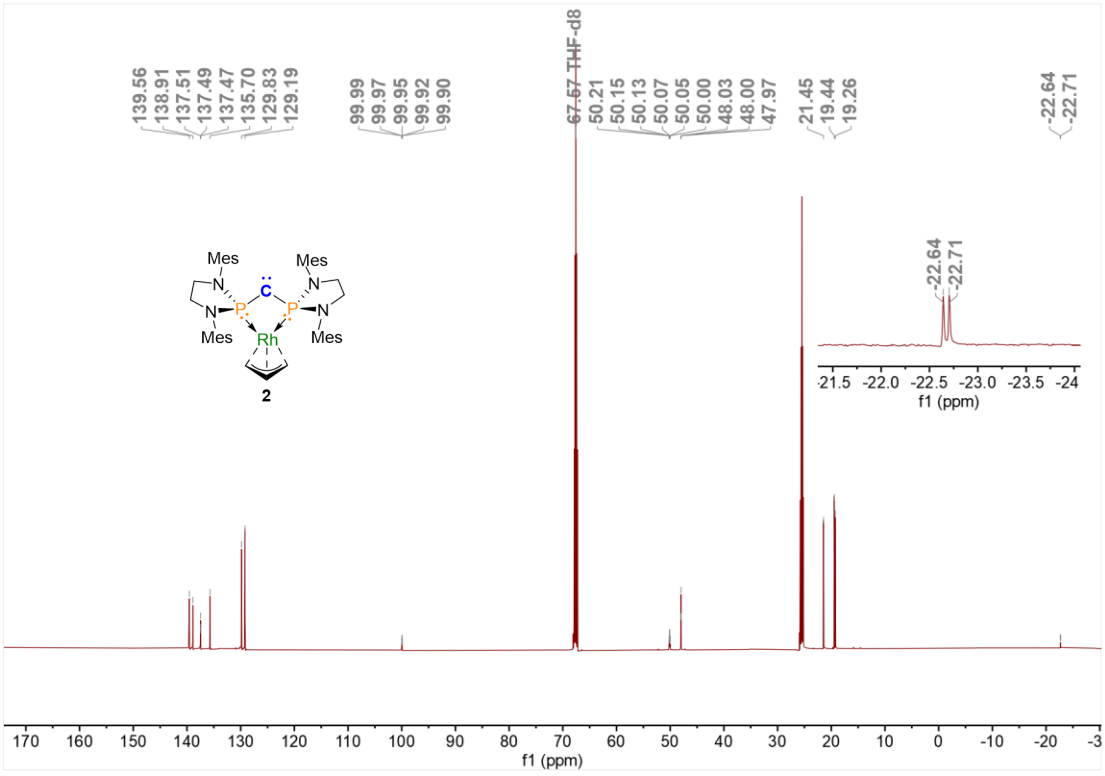

Fig. S4. ^{13}C{^{1}H} NMR spectrum of **2** (151 MHz, THF-d_8).

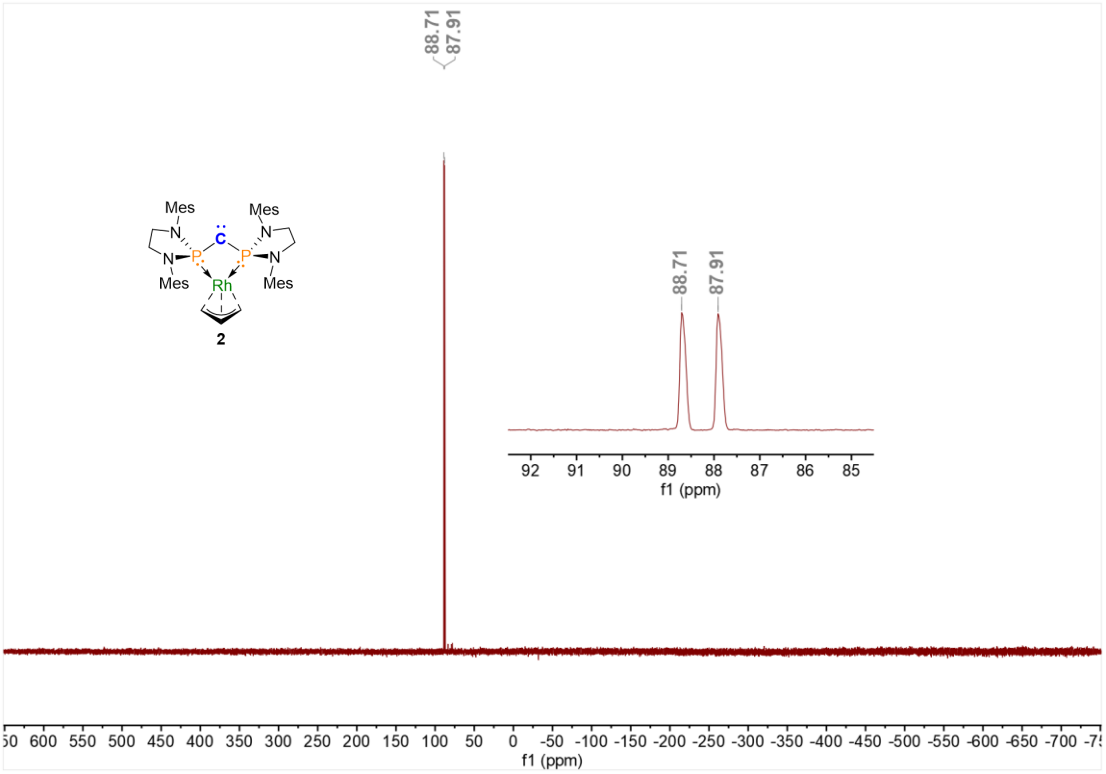

Fig. S5. ^{31}P NMR spectrum of **2** (243 MHz, THF-d_8).

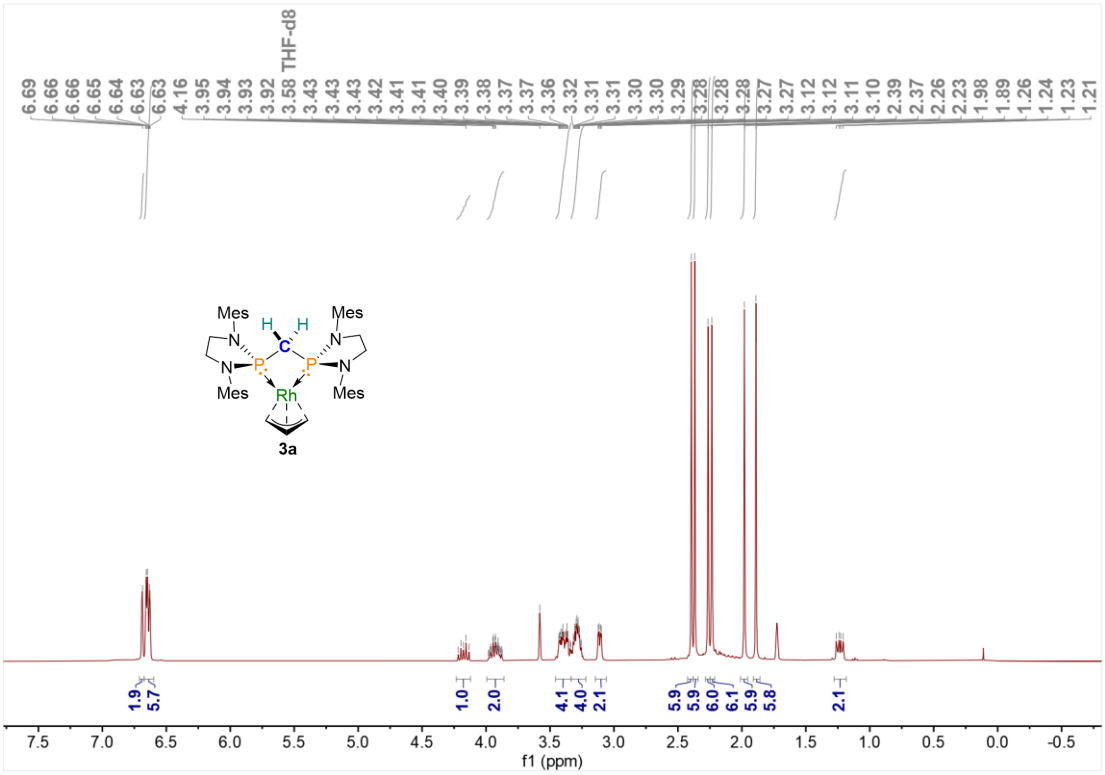

Fig. S6. ^{1}H NMR spectrum of **3a** (400 MHz, THF-d_8).

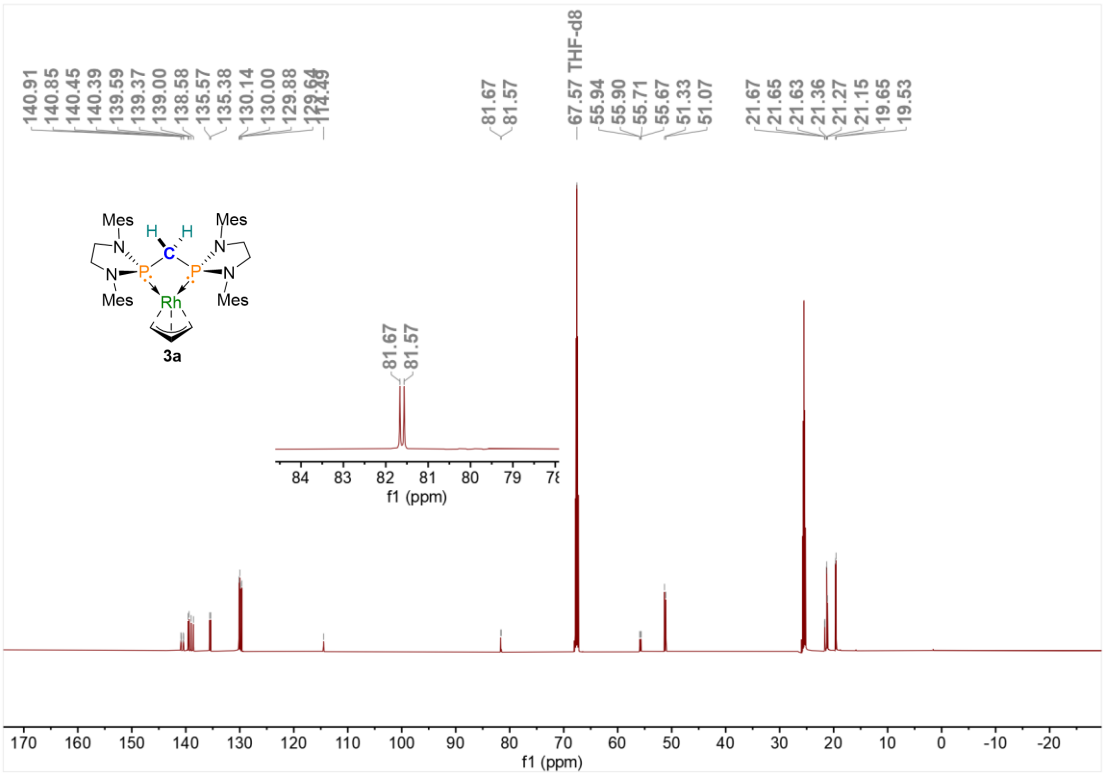

Fig. S7. $^{13}C\{^{1}H\}$ NMR spectrum of **3a** (151 MHz, THF-d_8).

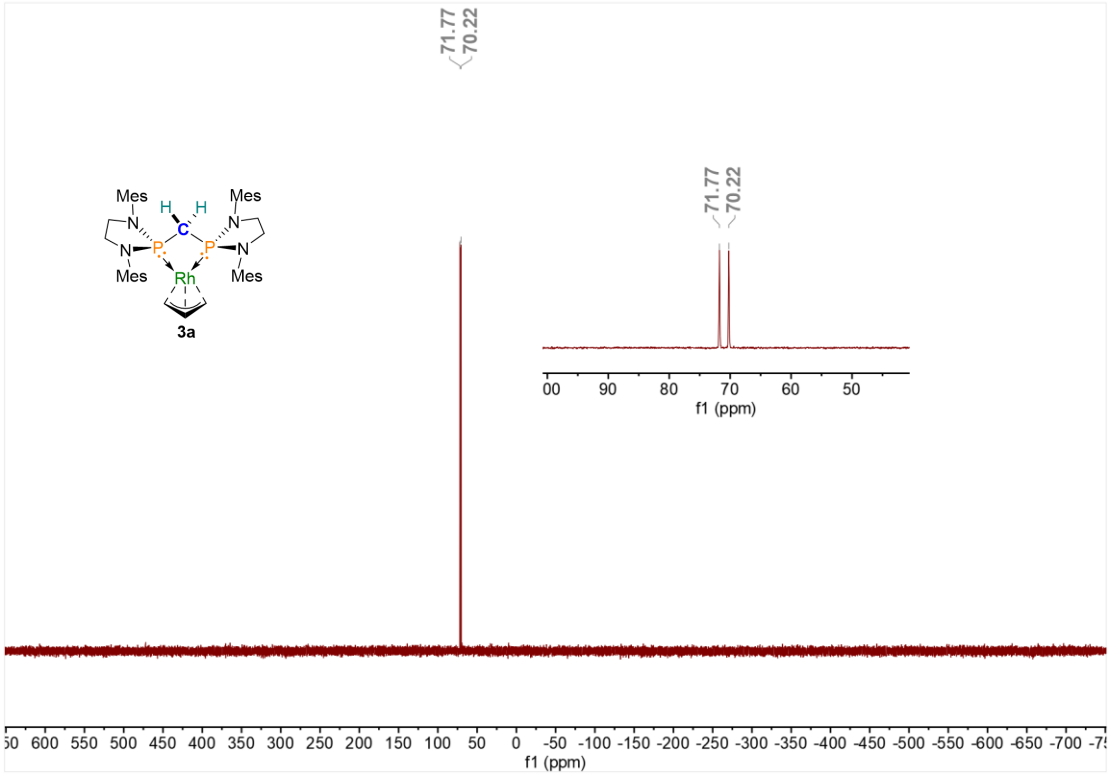

Fig. S8. ^{31}P NMR spectrum of **3a** (162 MHz, THF-d_8).

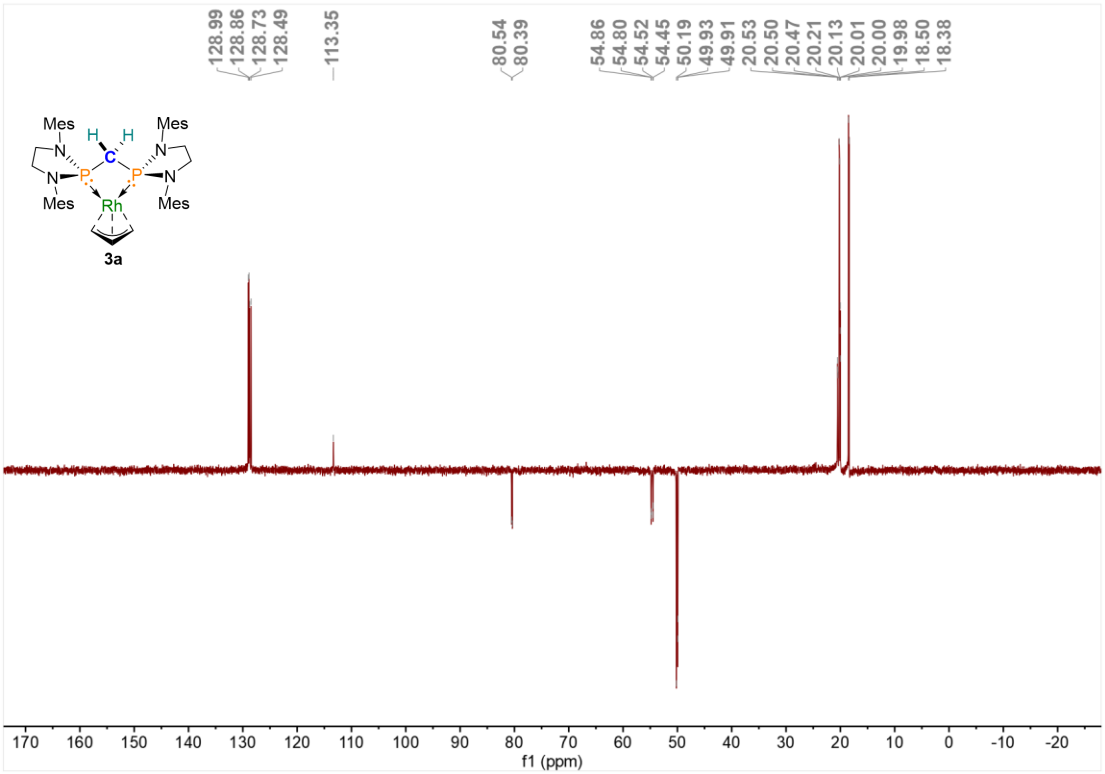

Fig. S9. DEPT-135 $^{13}C\{^{1}H\}$ NMR spectrum of **3a** (101 MHz, THF-d_8).

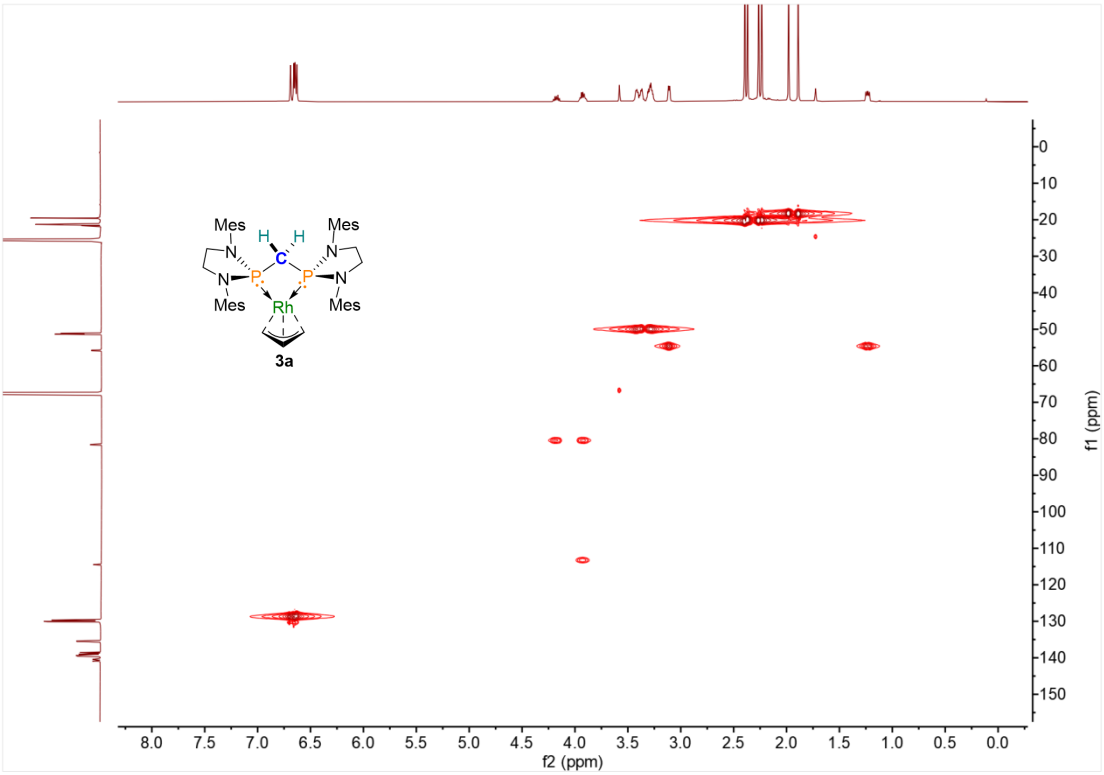

Fig. S10. ^{1}H-^{13}C HSQC spectrum of **3a** (600 MHz, THF-d_8).

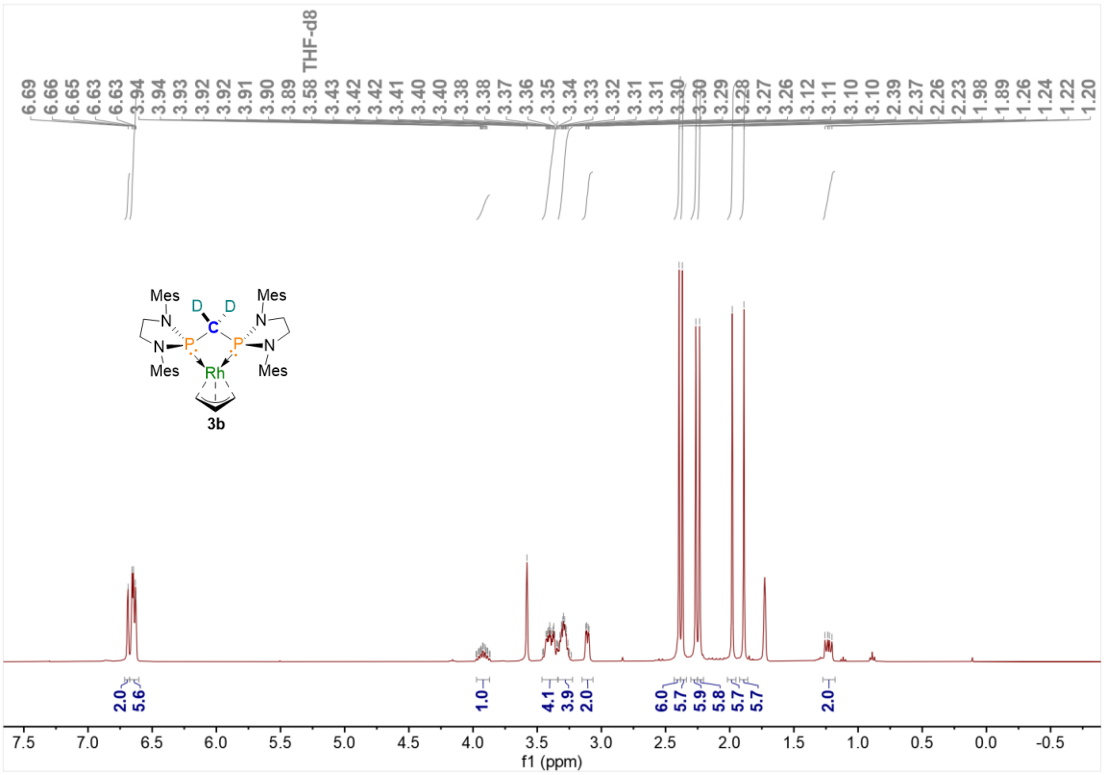

Fig. S11. ^{1}H NMR spectrum of **3b** (400 MHz, THF-d_8).

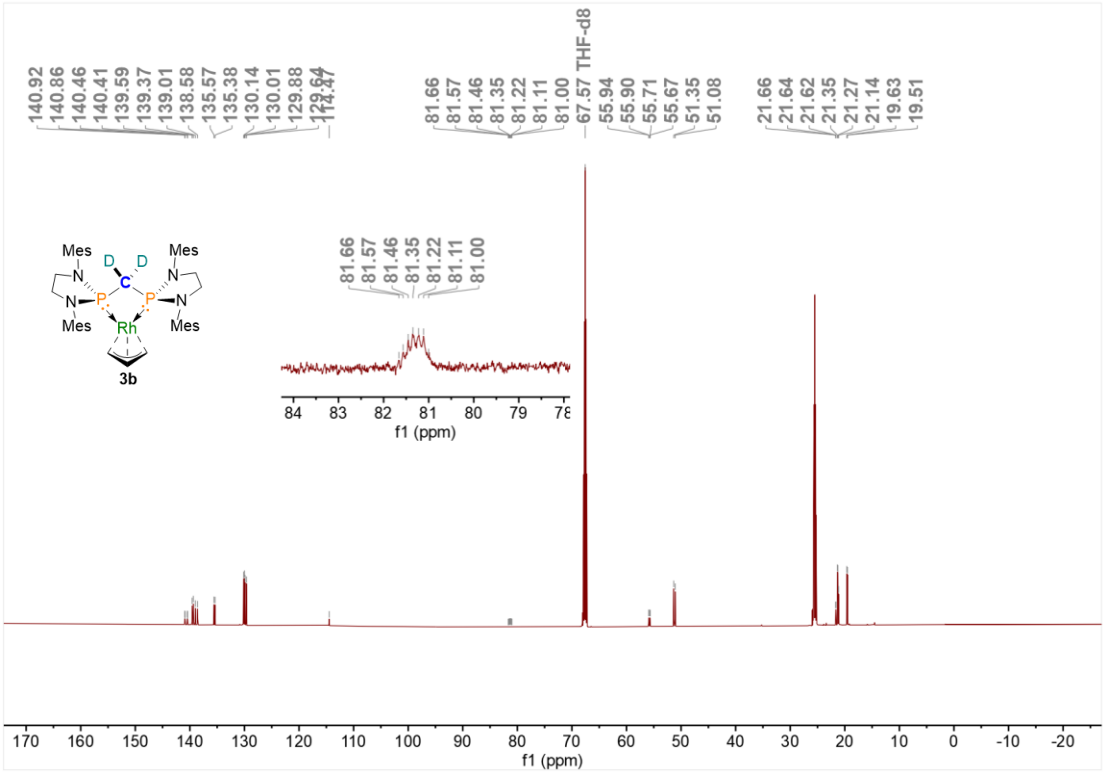

Fig. S12. ^{13}C{^{1}H} NMR spectrum of **3b** (151 MHz, THF-d_8).

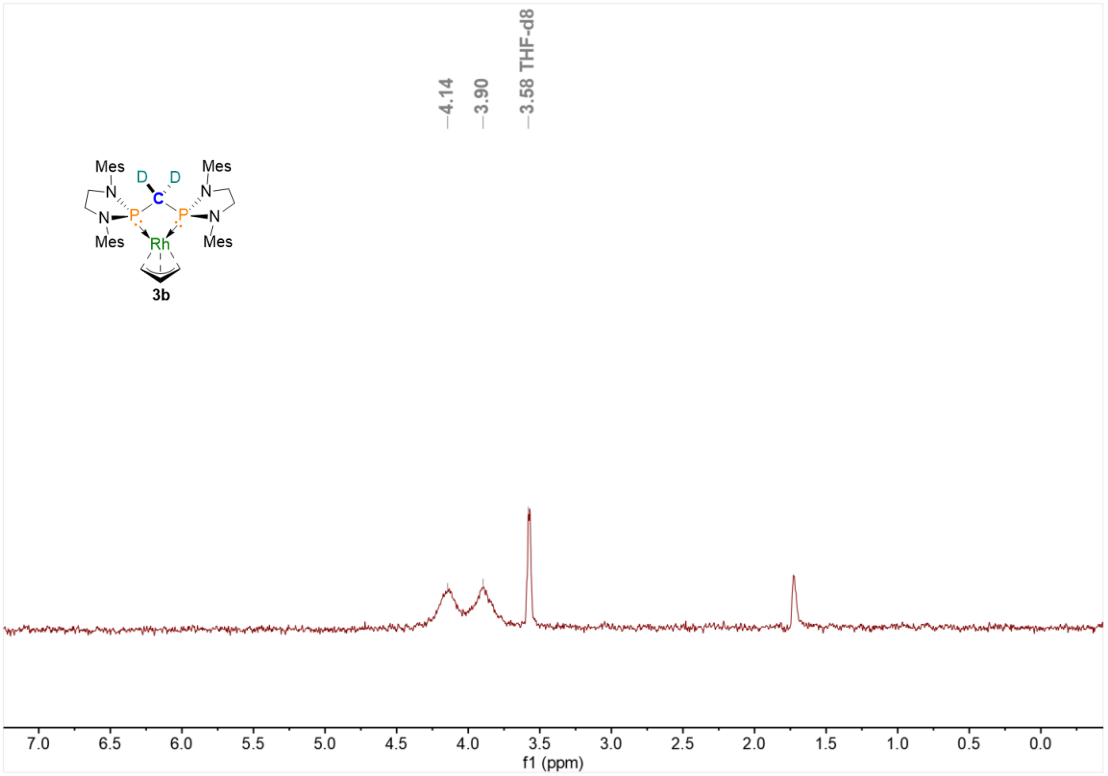

Fig. S13. ^{2}H NMR spectrum of **3b** (92 MHz, THF-d_8).

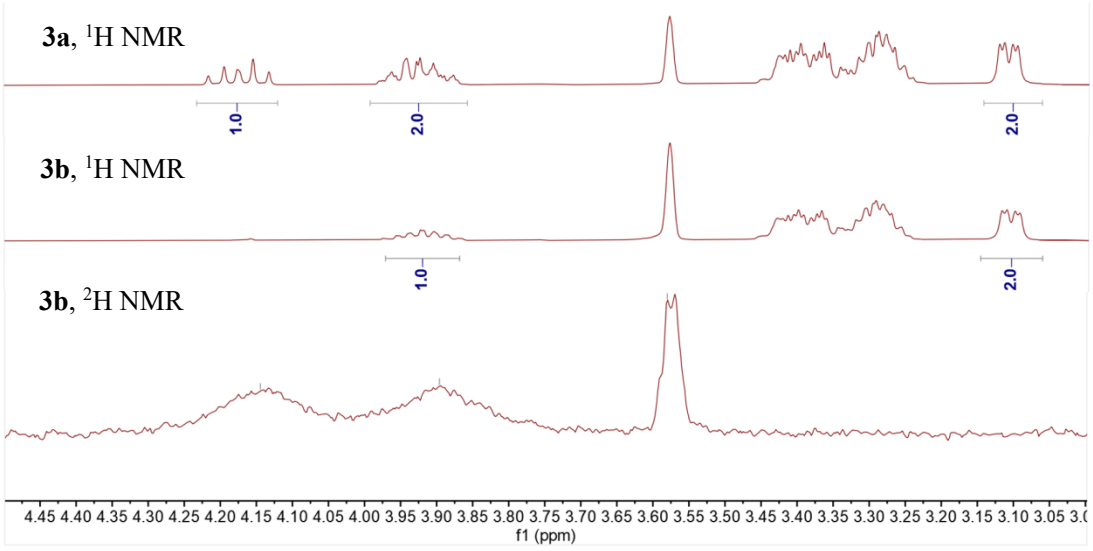

Fig. S14. Overlay of ^{1}H NMR spectrum of **3a**, **3b** and ^{2}H NMR spectrum of **3b**.

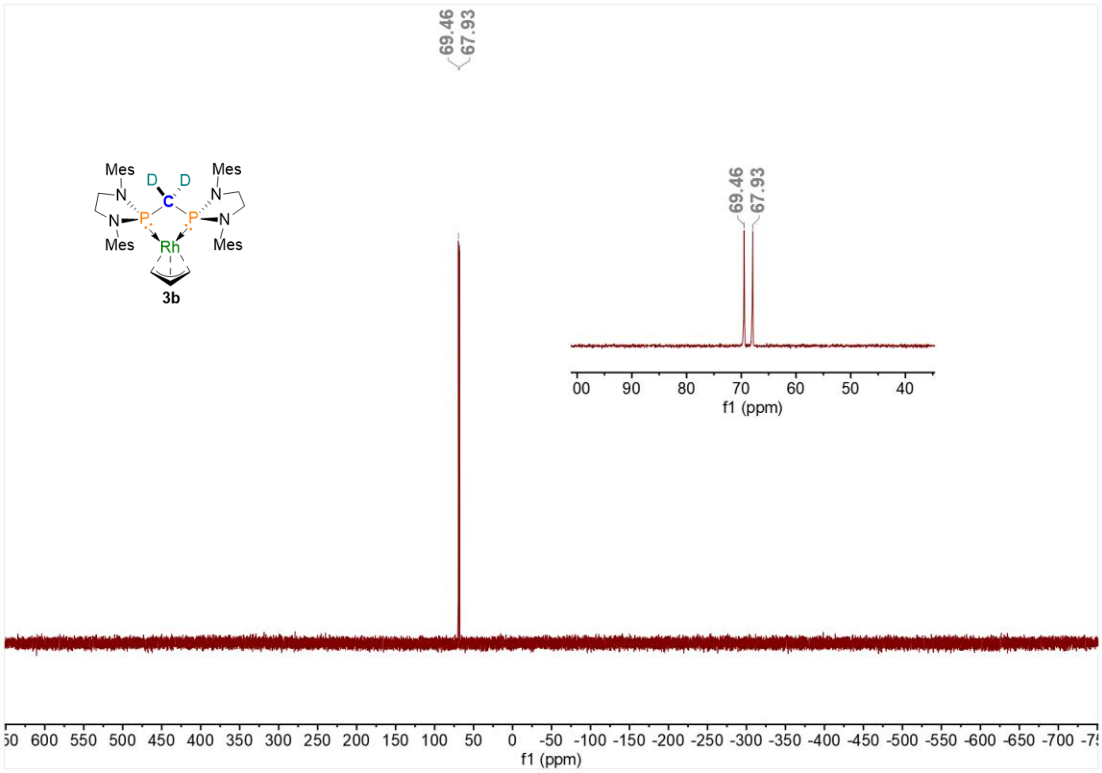

Fig. S15. ^{31}P NMR spectrum of **3b** (162 MHz, THF-*d*$_8$).

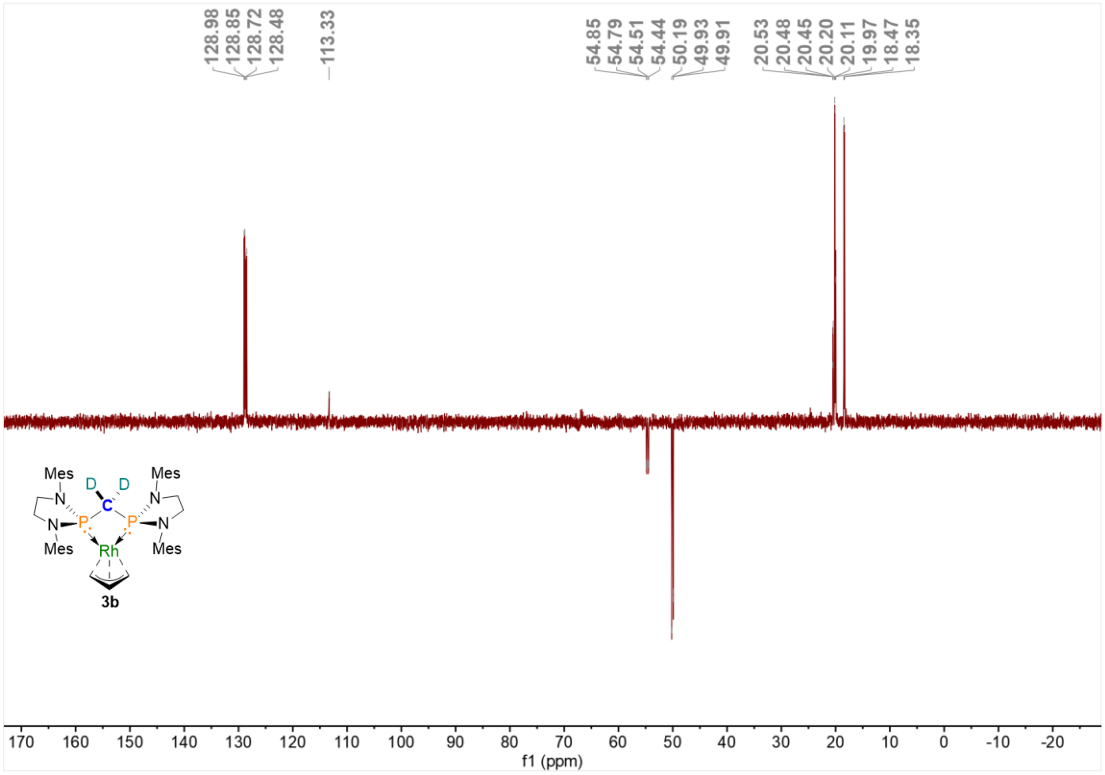

Fig. S16. DEPT-135 ^{13}C{^{1}H} NMR spectrum of **3b** (101 MHz, THF-*d*$_8$).

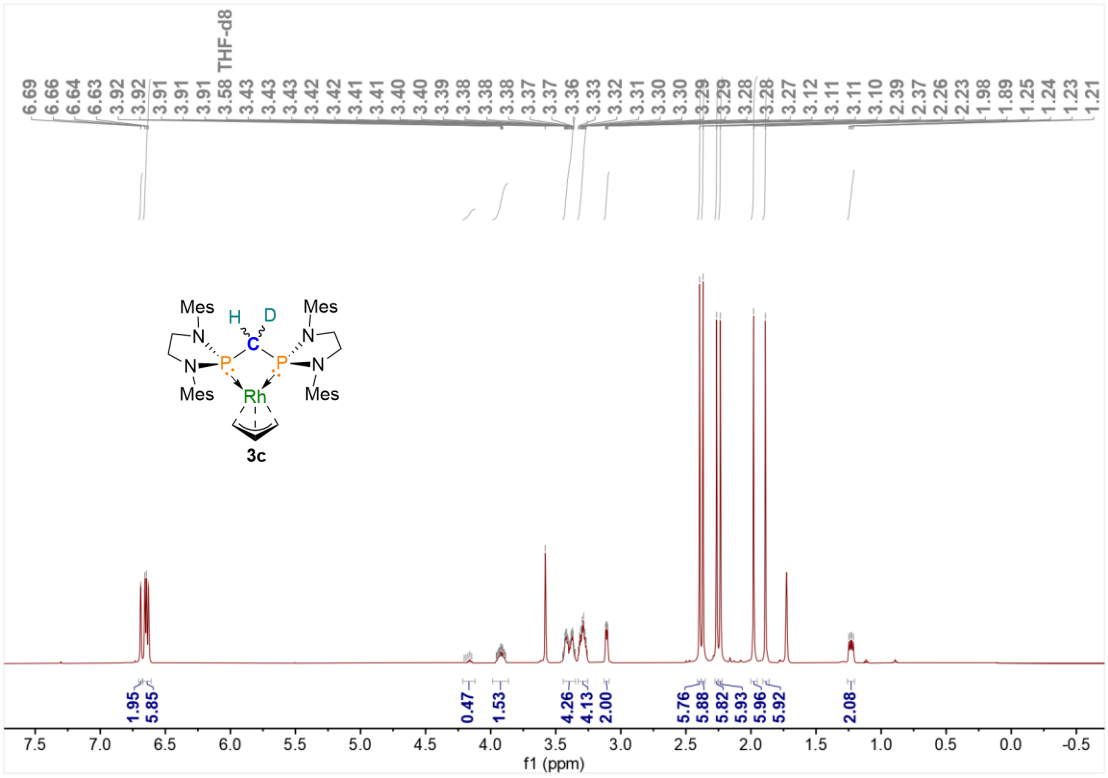

Fig. S17. ^{1}H NMR spectrum of **3c** (600 MHz, THF-d_8).

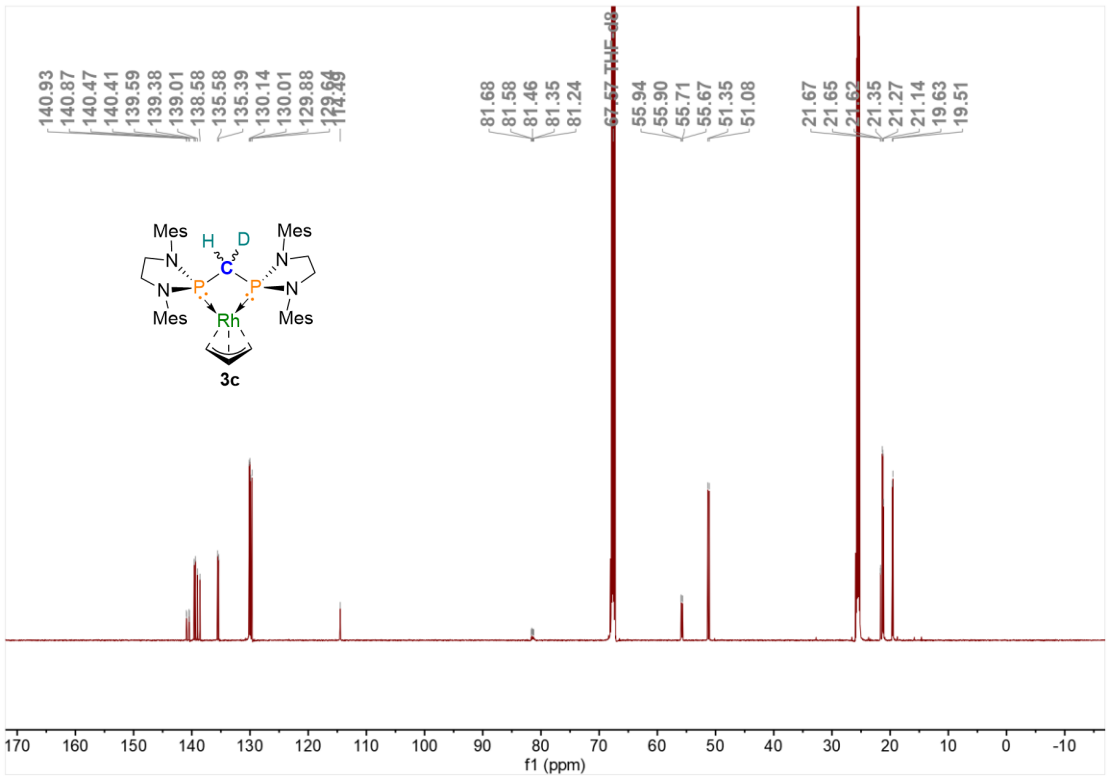

Fig. S18. ^{13}C{^{1}H} NMR spectrum of **3c** (151 MHz, THF-d_8).

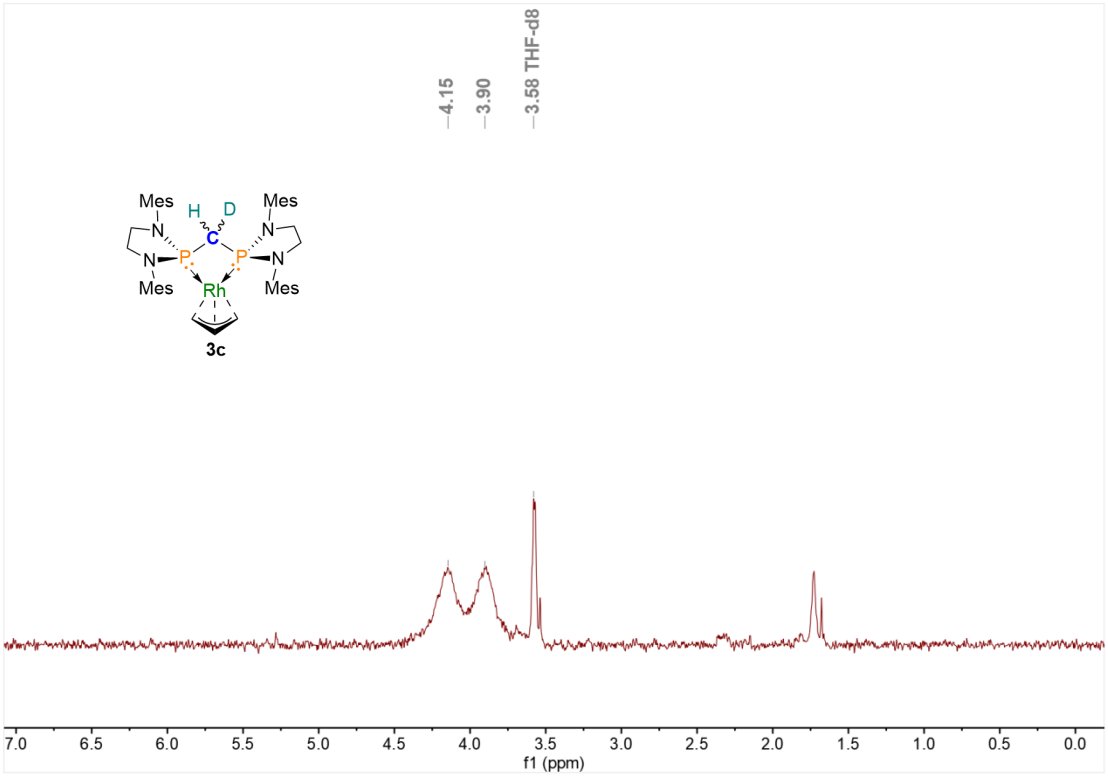

Fig. S19. ^{2}H NMR spectrum of **3c** (92 MHz, THF-d_8).

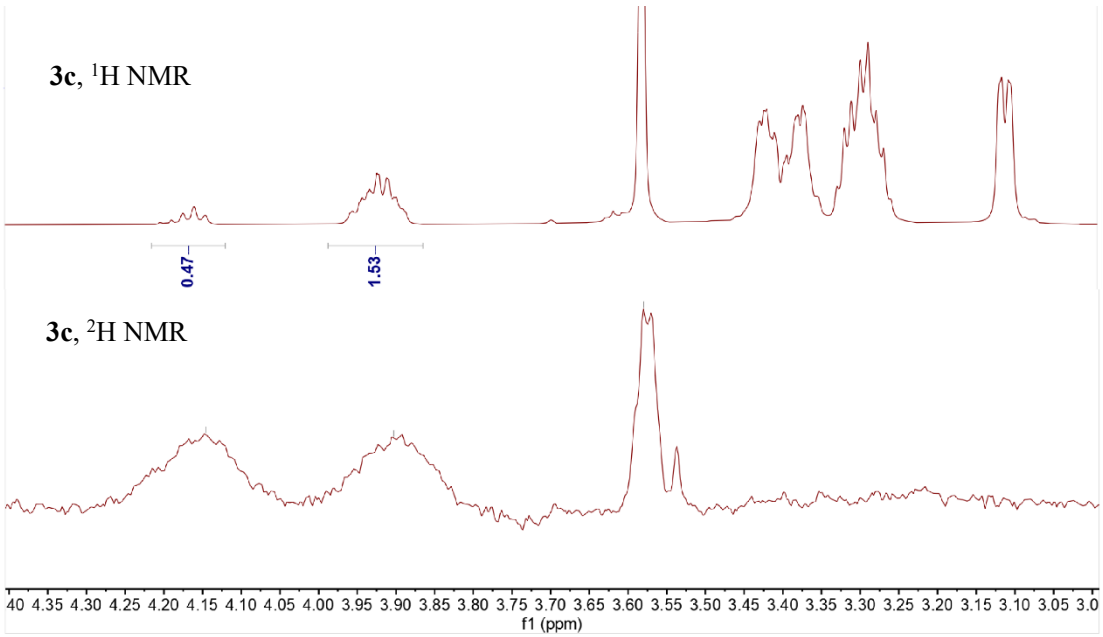

Fig. S20. Overlay of ^{1}H NMR spectrum and ^{2}H NMR spectrum of **3c**.

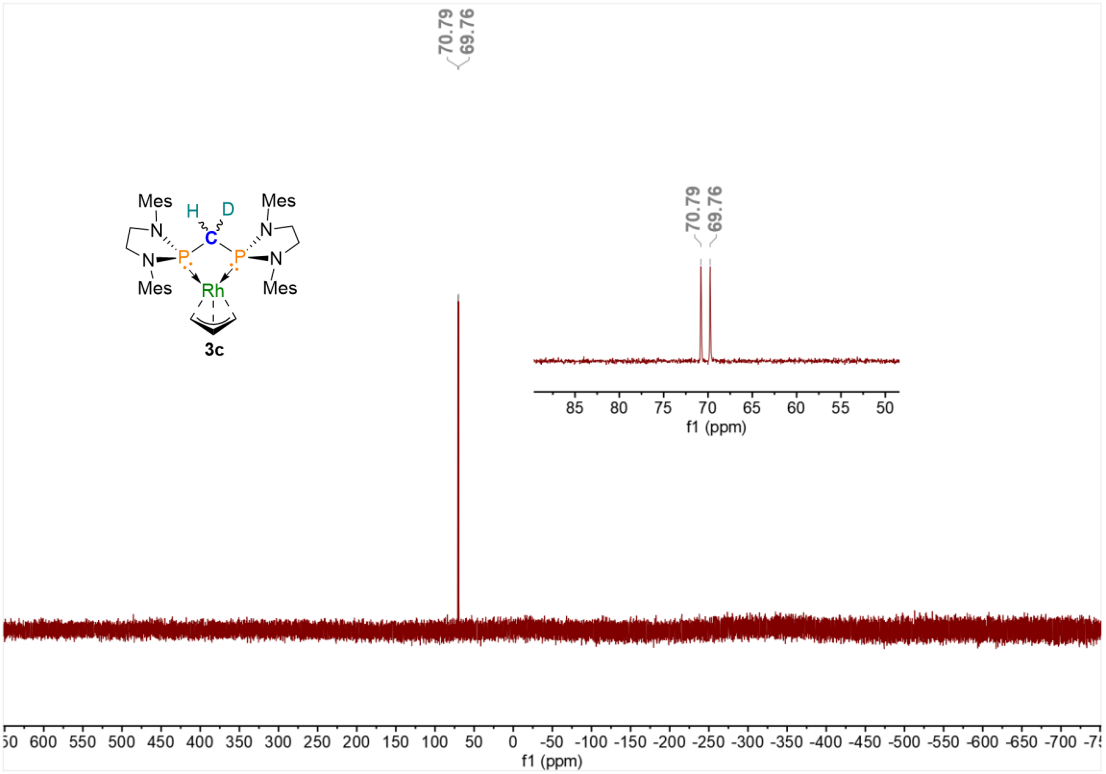

Fig. S21. ^{31}P NMR spectrum of **3c** (243 MHz, THF-d_8).

IV. HRMS Spectra

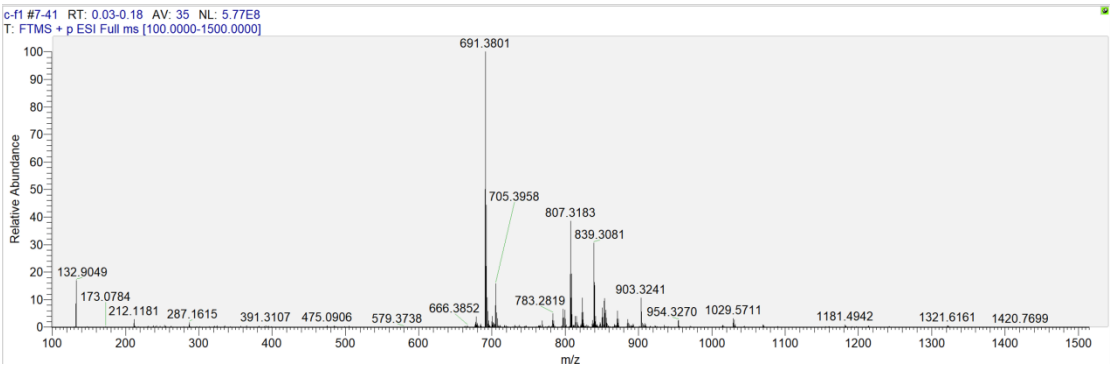

Fig. S22. Images for HRMS analysis of **2**. *HRMS* $[M+H]^+$ $C_{44}H_{58}N_4P_2Rh^+$ *calc. 807.3186 m/z, found 807.3183 m/z.*

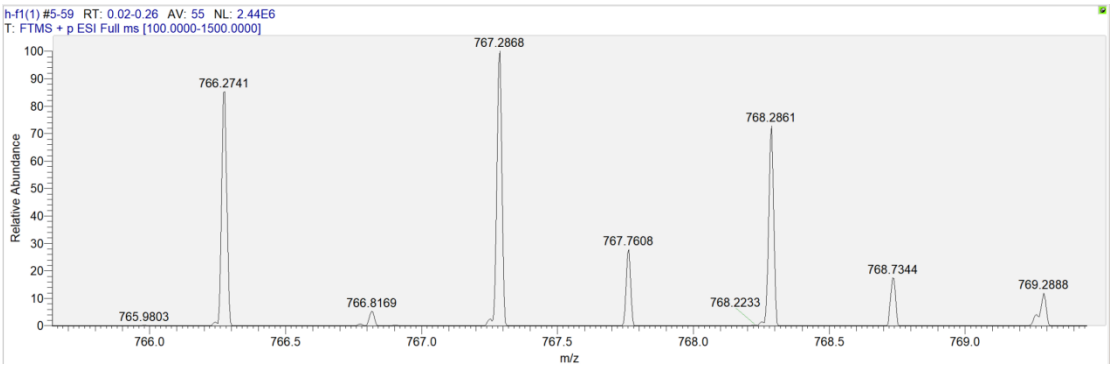

Fig. S23. Images for HRMS analysis of **3a**. *HRMS* $[M\text{-allyl}]^+$ $C_{41}H_{54}N_4P_2Rh^+$ *calc. 767.2873 m/z, found 767.2868 m/z.*

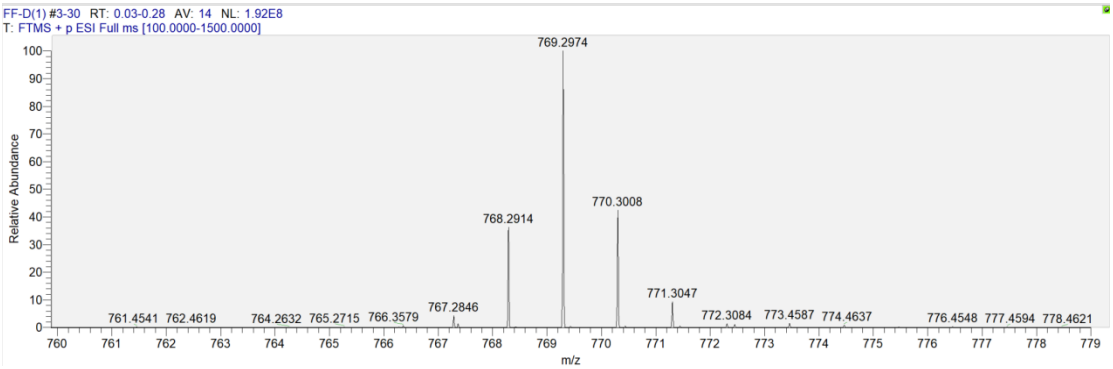

Fig. S24. Images for HRMS analysis of **3b**. *HRMS* $[M\text{-allyl}]^+$ $C_{41}H_{52}D_2N_4P_2Rh^+$ *calc. 769.2999 m/z, found 769.2974 m/z.*

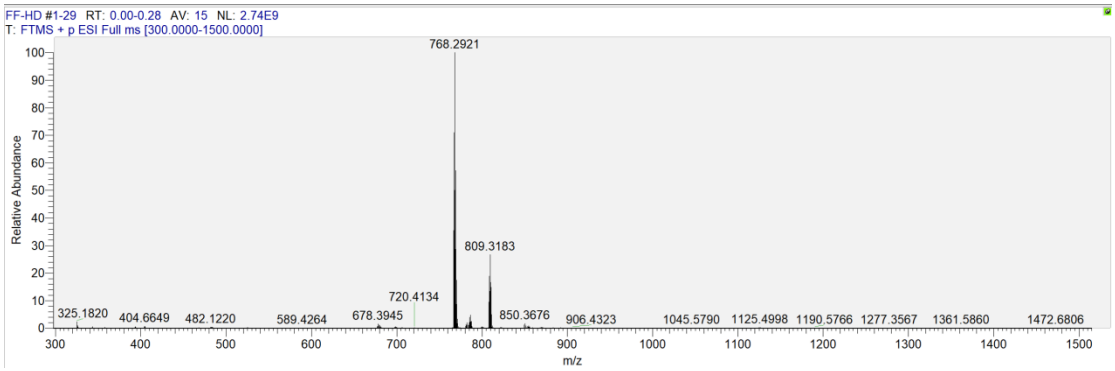

Fig. S25. Images for HRMS analysis of **3c**. *HRMS [M-allyl]$^+$ $C_{41}H_{53}DN_4P_2Rh^+$ calc. 768.2936 m/z, found 768.2921 m/z.*

V. X-ray Crystallographic Data

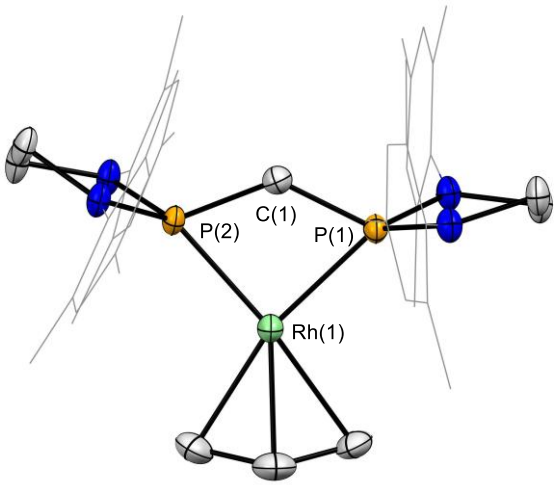

Fig. S26. Solid-state structure of **2**. Hydrogen atoms are omitted for clarity. Anisotropic displacement ellipsoids are set at the 40% probability level. Selected bond lengths (Å) and angles (°): P(1)−C(1) 1.6683(7), P(2)−C(1) 1.6896(7), Rh(1)−C(1) 2.2629(7), P(1)−C(1)−P(2) 132.53(4).

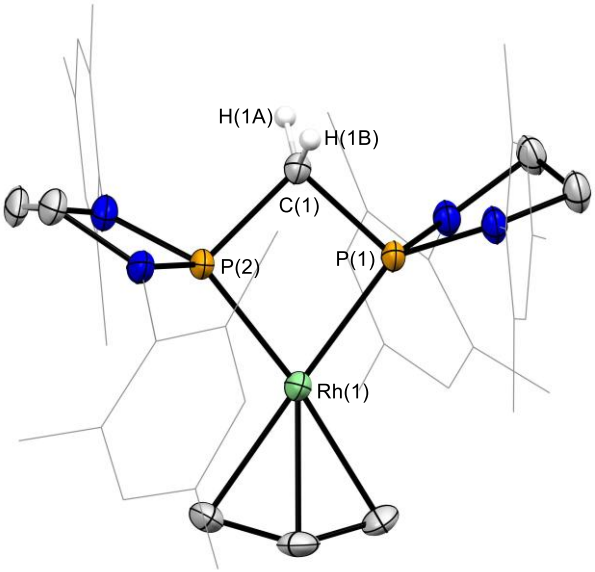

Fig. S27. Solid-state structure of **3a**. Hydrogen atoms are omitted for clarity. Anisotropic displacement ellipsoids are set at the 40% probability level. Selected bond lengths (Å) and angles (°): P(1)−C(1) 1.864(2), P(2)−C(1) 1.868(2), Rh(1)−C(1) 3.043(3), P(1)−C(1)−P(2) 92.59(11).

Table S1. Crystal data and structure refinement for **2.**

Identification code	**2**/ 2483382
Empirical formula	$C_{44}H_{57}N_4P_2Rh$
Formula weight	806.78
Temperature/K	100.00
Crystal system	monoclinic
Space group	$P2_1/c$
a/Å	13.5686(13)
b/Å	14.2506(13)
c/Å	21.239(2)
α/°	90
β/°	92.413(4)
γ/°	90
Volume/Å^3	4103.2(7)
Z	4
ρ_{calc}g/cm^3	1.306
μ/mm^{-1}	0.529
F(000)	1696.0
Crystal size/mm^3	0.3 × 0.28 × 0.2
Radiation	MoKα (λ = 0.71073)
2Θ range for data collection/°	4.516 to 90.54
Index ranges	$-27 \leq h \leq 27$, $-28 \leq k \leq 28$, $-42 \leq l \leq 42$
Reflections collected	370099
Independent reflections	34231 [R_{int} = 0.0736, R_{sigma} = 0.0321]
Data/restraints/parameters	34231/0/472
Goodness-of-fit on F^2	1.029
Final R indexes [I>=2σ (I)]	R_1 = 0.0318, wR_2 = 0.0760
Final R indexes [all data]	R_1 = 0.0456, wR_2 = 0.0828
Largest diff. peak/hole / e Å^{-3}	0.90/-1.27

Table S2. Crystal data and structure refinement for **3a.**

Identification code	**3a**/ 2483383
Empirical formula	$C_{47}H_{66}N_4P_2Rh$
Formula weight	851.88
Temperature/K	120.00
Crystal system	triclinic
Space group	P-1
a/Å	8.8844(8)
b/Å	10.5133(10)
c/Å	25.092(3)
α/°	82.486(4)
β/°	82.062(4)
γ/°	77.297(4)
Volume/Å^3	2252.2(4)
Z	2
ρ_{calc}g/cm^3	1.256
μ/mm^{-1}	2.731
F(000)	902.0
Crystal size/mm^3	0.2 × 0.1 × 0.05
Radiation	GaKα (λ = 1.34139)
2Θ range for data collection/°	7.54 to 118.79
Index ranges	$-11 \leq h \leq 11$, $-13 \leq k \leq 13$, $-32 \leq l \leq 32$
Reflections collected	59187
Independent reflections	9947 [R_{int} = 0.0638, R_{sigma} = 0.0449]
Data/restraints/parameters	9947/7/510
Goodness-of-fit on F^2	1.072
Final R indexes [I>=2σ (I)]	R_1 = 0.0405, wR_2 = 0.0983
Final R indexes [all data]	R_1 = 0.0540, wR_2 = 0.1046
Largest diff. peak/hole / e Å^{-3}	0.78/-1.09

VI. Photophysical Data

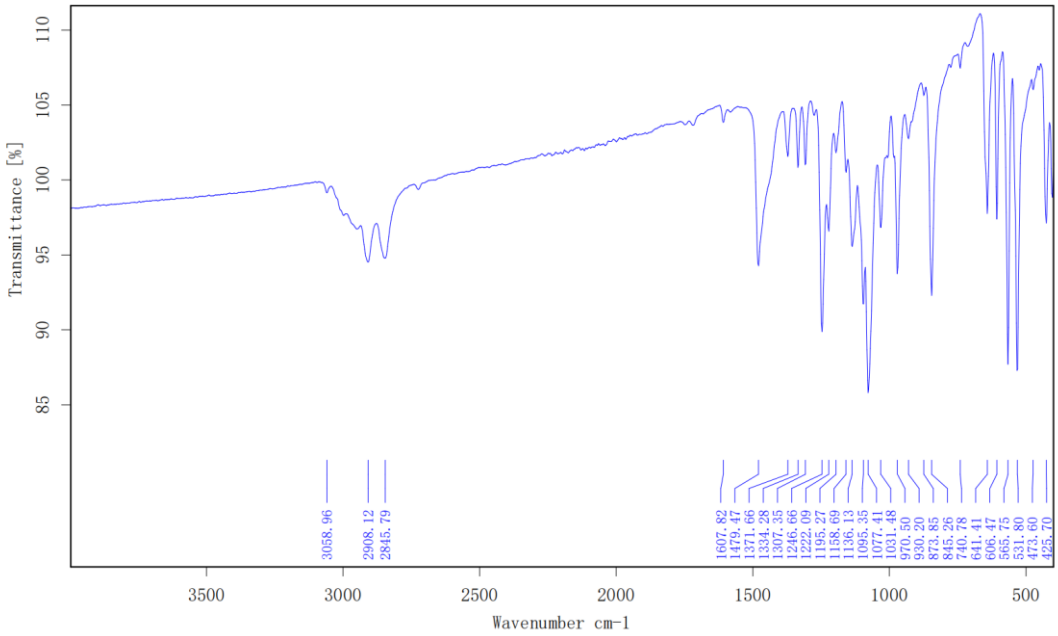

Fig. S28. Infrared spectrum of **2**.

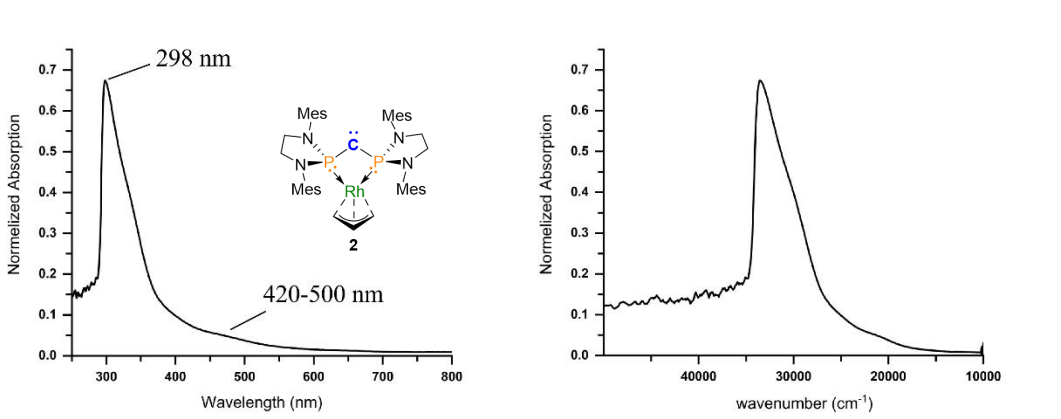

Fig. S29. UV-Vis spectrum of **2** in THF ($2*10^{-4}$ M). Linear legend construction based on wavelength, frequency (wavenumber), respectively.

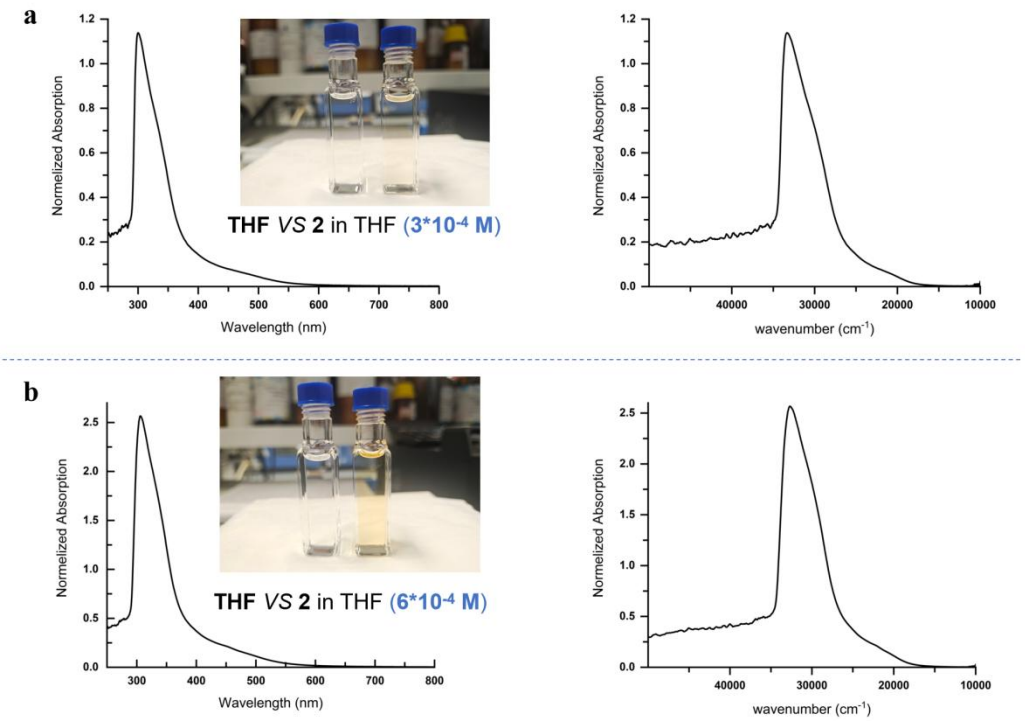

Fig. S30. Comparative UV-Vis results for samples with different concentrations. **a**, **2** in THF ($3*10^{-4}$ M). **b**, **2** in THF ($6*10^{-4}$ M).

VII. Kinetic Experiments

7.1 Time-course kinetics for D_2.

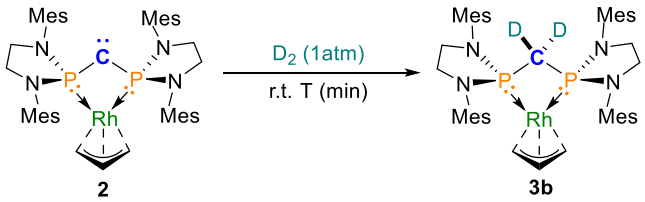

In a dried Schlenk tube, a solution of **2** (500 μL, 0.02 M in C_6D_6) was combined with 1,3,5-trimethoxybenzene (100 μL, 0.05 M in C_6D_6). The mixture was degassed by 3–5 freeze–pump–thaw cycles and then backfilled with 1 atm of D_2 at 10 °C. The reaction mixture was warmed to room temperature and stirred for a preset time. For each time point, a reaction was set up in parallel following the same protocol (including one "t = 0" control in which D_2 was not introduced). The concentrations of **2** and **3b** were determined by integrating well-resolved methyl resonances of the mesityl substituents relative to the methyl resonances of the internal standard, taking into account the known concentration and the number of contributing protons for each signal.

Table S3. Full time course tracking the evolution of **2** and **3b**.

Time (min)	**3b** Concentration (M)	**2** Concentration (M)
0	0	0.01666
60	0.00044	0.01567
120	0.00100	0.01533
180	0.00144	0.01500
240	0.00279	0.01350
360	0.00439	0.01167
480	0.00560	0.01017
600	0.00641	0.00933
780	0.00740	0.00817
960	0.00960	0.00567
1140	0.01040	0.00467
1320	0.01260	0.00217
1440	0.01400	0

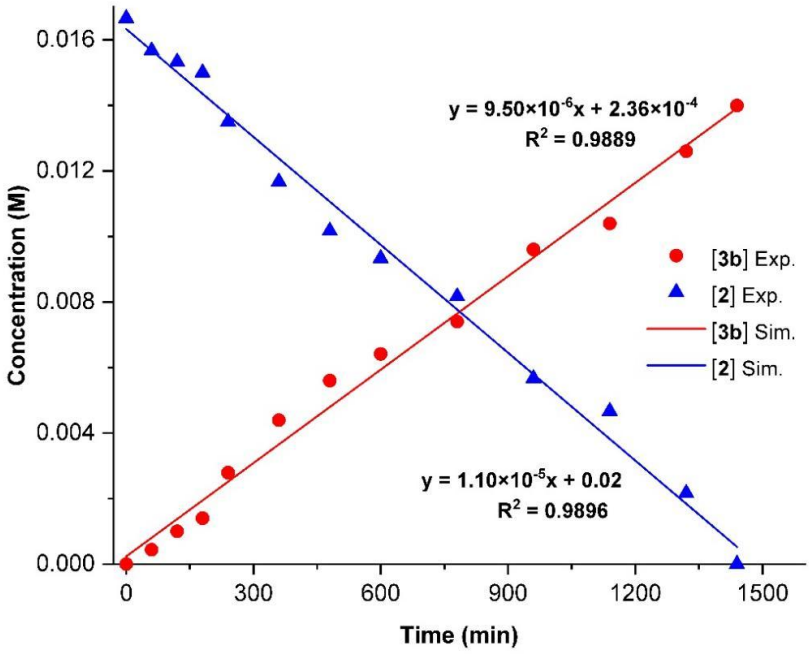

Fig. S31. Experimental and simulated concentration profiles of complex **2** (blue triangles) and **3b** (red circles).

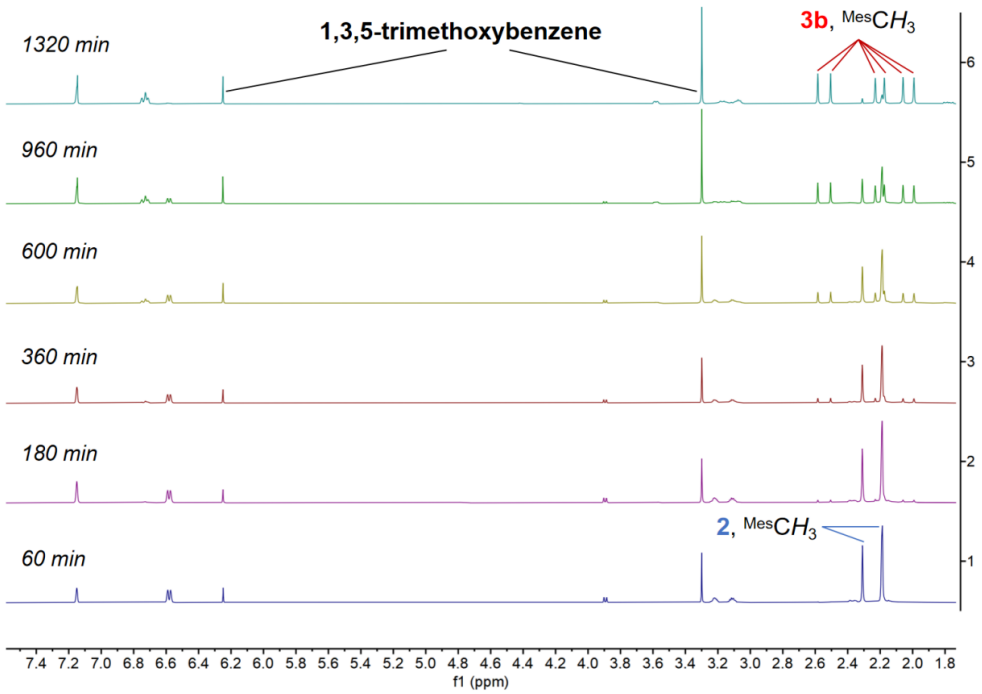

Fig. S32. Partial ^{1}H NMR spectra at various times. *At the initial stage of the reaction, the mesityl (Mes) methyl protons of starting material **2** showed two sets of signals with an integral ratio of 1:2 (12H:24H). As the reaction proceeded, product **3b** was gradually formed and accumulated; correspondingly, the Mes methyl protons of **3b** exhibited six sets of signals in a 1:1:1:1:1:1 (6H:6H:6H:6H:6H:6H) integral ratio, which is consistent with its structural characteristics.*

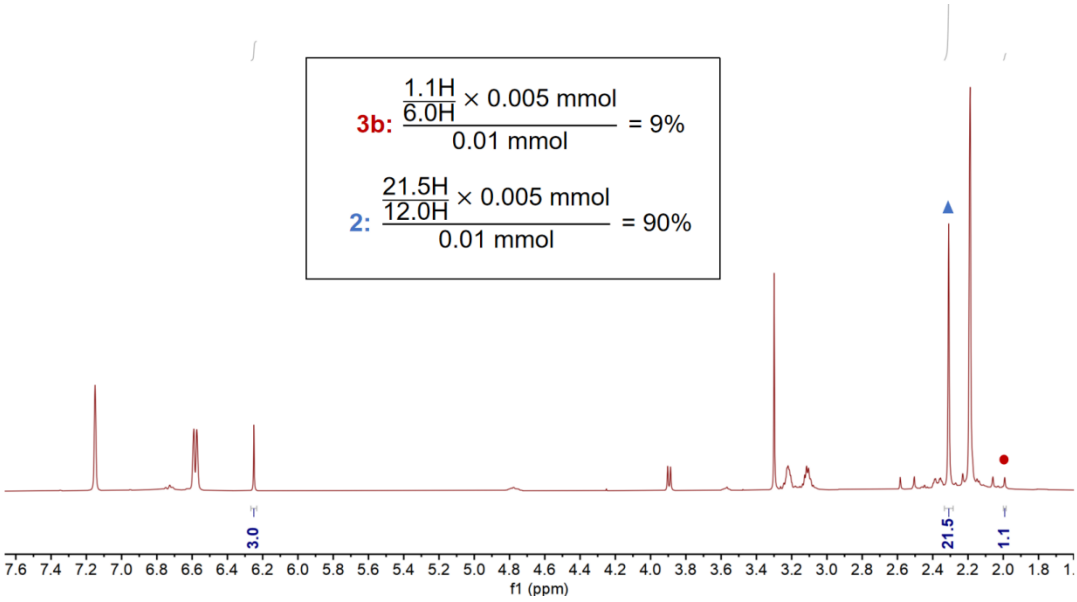

Fig. S33. ^{1}H NMR Spectrum of the reaction after 180 minutes. *The yield of product **3b** and the remaining percentage of starting material **2** were quantified by ^{1}H NMR spectroscopy using an internal standard with a known number of aryl protons (3H). First, the well-resolved mesityl methyl proton signals of **2** and **3b** in the reaction mixture were integrated separately. The normalized value was divided by the theoretical number of mesityl methyl protons per mole of the corresponding compound, multiplied by the molar amount of the internal standard, and finally divided by the initial molar amount of starting material **2** to yield the yield of **3b** and the remaining percentage of **2**.*

7.2 KIE determination from the initial-rate regime.

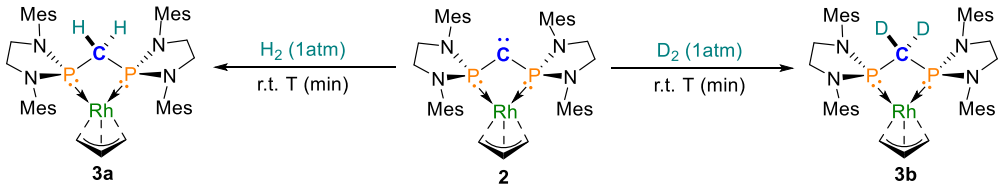

Guided by the full D_2 time-course experiment above, we next performed parallel kinetic runs under H_2 and D_2 specifically in the low-conversion regime to extract the KIE. Using the same quantitative ^{1}H NMR protocol (same solvent, internal standard, degassing/backfilling procedure, temperature profile, and mixing conditions), aliquots were analyzed at 60, 90, 120, and 150 min, and the concentrations of products **3a** and **3b** were determined from their methyl integrals relative to the internal standard.

Over this ≤10% conversion interval, the product concentration increases linearly with time for both isotopologues. Therefore, we obtained the initial-rate slopes ($v_{0,H} = 1.28\times10^{-5}$ and $v_{0,D} = 8.43\times10^{-6}$) by linear regression of [**3a**] or [**3b**] versus time, and defined the kinetic isotope effect as:

$$\mathrm{KIE} = \frac{k_H}{k_D} \approx \frac{v_{0,H}}{v_{0,D}}$$

From the fitted slopes, we obtain KIE = 1.52 at room temperature (298 K) under 1 atm of gas.

Table S4. Kinetic data of **3a** and **3b** at varying reaction times.

Time (min)	**3a** Concentration (M)	**3b** Concentration (M)
60	0.00056	0.00044
90	0.00089	0.00075
120	0.00130	0.00100
150	0.00170	0.00120

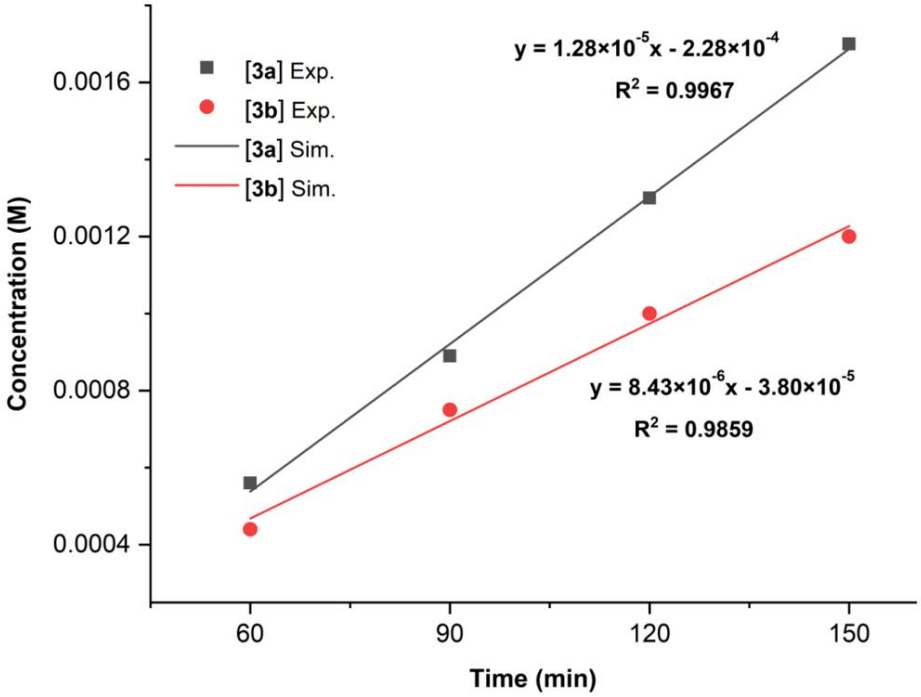

Fig. S34. Experimental and simulated concentration profiles of **3a** (gray squares) and **3b** (red circles). *A negative intercept is observed, which we attribute to the sampling delay inherent in the experimental procedure.*

VIII. Computational Details

All molecular geometry optimizations were carried out with the Gaussian 16 software package*(3)* at the BP86-D3(BJ)/def2-SVP level in the gas phase under 1 atm and 298K.*(4-8)* Vibrational frequency calculations were conducted at the same level to verify the character of the optimized geometries, confirming them as either local minima (no imaginary frequencies) or transition states (one imaginary frequency). Single-point energy calculations were subsequently carried out on the optimized geometries at the BP86-D3(BJ)/def2-TZVP level in the gas phase to determine the relative energies. The transition states were further validated by analyzing normal mode vibrational vectors and conducting the intrinsic reaction coordinate (IRC) calculations.(*9,10*) Natural bond orbital (NBO) calculations were implemented with NBO 7.0 program*(11)* a at the BP86-D3(BJ)/def2-SVP level, and intrinsic bond orbitals (IBOs) were performed with the ORCA 5.0.3 program package*(12)* at the same level. Optimized structures were visualized by the CYLview,*(13)* Chemcraft*(14)* or IBOview program.*(15)* Time-dependent density functional theory (TD-DFT) calculations were executed at the BP86-D3(BJ)/def2-TZVP level, and the results were visualized with the GaussSum program*(16)*. The solvation model based on density (SMD)*(17)* was employed for the TD-DFT calculations with THF as the solvent. The electron localization function (ELF) analyses*(18)* were carried out using Amsterdam Modeling Suite*(19)* at the BP86-D3(BJ)/TZP level. Heavy-atom root-mean-square deviation (RMSD) calculations were performed with Chemcraft program.*(20)*

8.1 Geometry optimization and singlet–triplet energy gap of **2**.

Table S5. Selected bond lengths (Å) and angles (°) for the solid and the optimized structures of **2**.

	Solid structure	Optimized structure
P(1)–C(1)	1.6683(7)	1.71213
P(2)–C(1)	1.6896(7)	1.68205
Rh(1)–C(1)	2.2629(7)	2.29438
P(1)–Rh(1)	2.2084(2)	2.23202
P(2)–Rh(1)	2.2107(2)	2.23972
P(1)–C(1)–P(2)	132.53(4)	132.28848
C(1)–P(1)–Rh(1)	69.84(3)	69.72016
C(1)–P(2)–Rh(1)	69.46(3)	69.96403
P(1)–Rh(1)–P(2)	88.151(10)	87.92500

Table S6. Singlet–triplet energy gap ($\Delta E_{S\text{-}T}$) of **2.**

	Electronic Energy (Hartree)	$\Delta E_{S\text{-}T}$ (kcal/mol)
2$_{\_triplet}$	-2723.694346	0.00000
2$_{\_singlet}$	-2723.729190	-21.86547

8.2 TDDFT calculations of **2**.

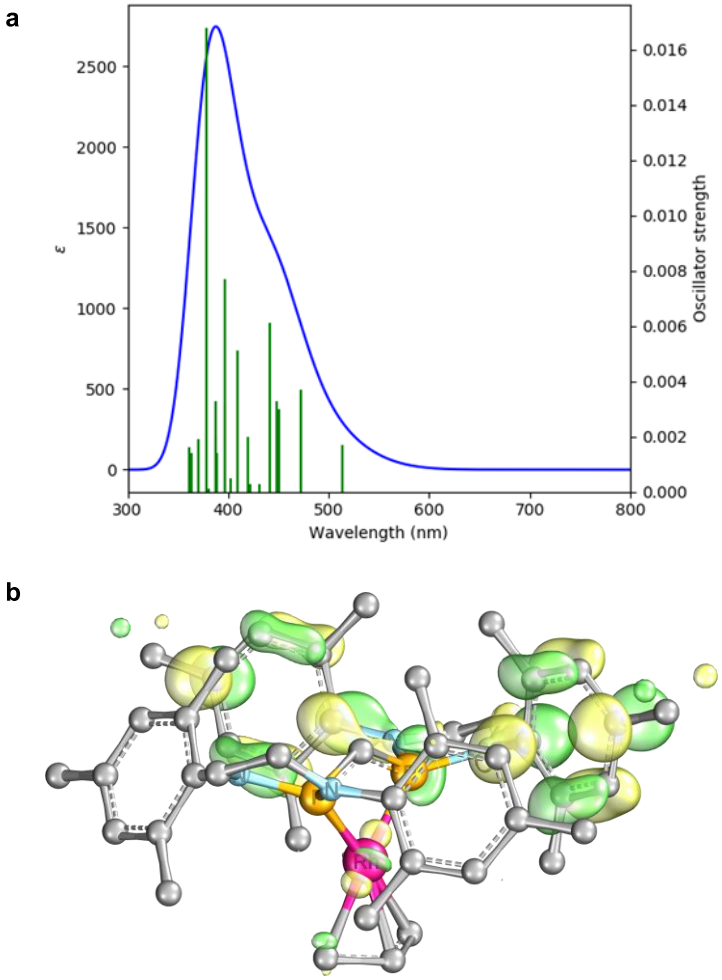

Fig. S35. **a**, Simulated UV-vis spectrum of **2** from TD-DFT calculations. The absorptions at 513 nm and 472 nm are mainly attributed to the transitions (HOMO→LUMO, 99%) and (HOMO→LUMO+1, 99%), respectively. **b**, LUMO+1 orbital of **2**.

8.3 NMR calculations

At the CPCM-wB97X-D3/def2TZVP level of theory, the computed chemical shift for the carbene carbon in **2** is –27.0 ppm (Table S7), which is in good agreement with the experimental value of –22.7 ppm.

It is well established that, for nuclei involved in bonding schemes dominated by p orbitals, the paramagnetic contribution (σ_{para}) plays an important role in determining chemical shift. In conventional NHCs, the characteristic high-frequency ^{13}C resonances are generally attributed to strong paramagnetic deshielding.

To elucidate why the carbene carbon in **2** resonates at an unusually low frequency, we compared its magnetic shielding components with those of IAd (1,3-di(adamantyl)-1,3-dihydro-2*H*-imidazol-2-ylidene) (Fig. S37). The shielding tensors were decomposed into their diamagnetic (σ_{dia}) and paramagnetic (σ_{para}) contributions along the three principal axes (Tables S8 and S9).

For IAd, the diamagnetic shielding is positive but relatively uniform, with σ_{dia} values ranging from 254.9 to 277.9 ppm, whereas the paramagnetic deshielding is pronounced along all three axes (σ_x = −287.0 ppm, σ_y = −110.5 ppm, σ_z = −512.3 ppm), resulting in an overall σ_{iso} of −33.7 ppm. In contrast, **2** exhibits a dual effect: not only is the paramagnetic deshielding substantially attenuated (σ_x = −173.1 ppm, σ_y = −109.7 ppm, σ_z = +77.8 ppm), but the diamagnetic shielding is also moderately enhanced, with σ_{dia} values ranging from 253.6 to 304.0 ppm. Together, these effects lead to a markedly larger isotropic shielding (σ_{iso} = 207.4 ppm).

Consequently, the unusually low-frequency ^{13}C resonance of the carbene center in **2** originates from the combined influence of diminished paramagnetic deshielding and modestly strengthened diamagnetic shielding, resulting in a highly shielded electronic environment that stands in sharp contrast to that of conventional NHCs.

To further elaborate on the paramagnetic (de)shielding contributions of both **2** and IAd, we conducted a detailed analysis of their magnetic couplings. The overall paramagnetic (de)shielding is a sum of the major magnetic couplings, which are accompanied by many smaller couplings; however, for clarity, we focused on the most significant contributions.

In the case of IAd, all major magnetic couplings contribute to paramagnetic deshielding of the carbene carbon, with the dominant contribution arising from the HOMO→LUMO+2 transition (−167.2 ppm, accounting for 32.6% of σ_z; Fig. S38). This strong and uniformly deshielding pattern is characteristic of conventional NHCs and underlies their high-frequency ^{13}C resonances.

In sharp contrast, the situation in **2** is qualitatively different (Fig. S39). Of the four largest magnetic couplings, three contribute to paramagnetic shielding, while only one gives rise to a minor deshielding contribution. These major transitions contribute +49.0, +63.4, and +23.6 ppm, respectively, with the HOMO–16→LUMO and HOMO–2→LUMO excitations accounting for 63.0% and 81.5% of σ_z. Notably, all four dominant couplings involve orbitals with substantial mixed C/Rh character, indicating that metal–carbene orbital interactions play a decisive role in shaping the magnetic response at the carbene carbon.

Taken together, these results show that the unusually low-frequency ^{13}C NMR resonance of the rhodadiphosphinocarbene does not arise solely from its unconventional $\sigma^0\pi^2$ electronic configuration, but is critically reinforced by Rh participation, which reshapes the key orbital transition manifold governing paramagnetic (de)shielding.

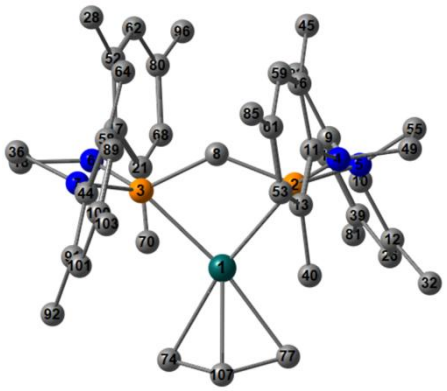

Fig. S36. Optimized geometry of **2**.

Table S7. Computed ^{13}C NMR chemical shift (ppm) of the carbene carbon in **2**, with C(107) (carbon of allylic CH) taken as the reference.

Atomic number	Calculated magnetic shielding tensor (ppm)	^{13}C NMR chemical shifts (ppm)
107	80.415	100.0 (experiment value)
8	207.444	**-27.0** (calculated value)

The geometries of **2** and IAd (1,3-di(adamantyl)-1,3-dihydro-2*H*-imidazol-2-ylidene, Fig. S37) were first optimized at the BP86-D3(BJ)/def2-SVP level using the Gaussian 16 software package*(3)*. The resulting structures were then adopted as input for the calculations of ^{13}C NMR shielding shift using the ORCA 5.0.3 program package*(12)*, with the range-separated hybrid functional wB97X-D3*(21)* combined with the def2-TZVP basis set. The conductor-like polarizable continuum model (CPCM) *(22-25)* was utilized to account for solvation effects, with THF as the solvent. The absolute shielding tensor of the carbene center obtained from these calculations were then converted to chemical shifts (δ ppm) using eq. 1:

$$\delta_{sample} = \sigma_{ref} - \sigma_{sample} + \delta_{ref\,(exp.)} \qquad (1)$$

Herein, σ_{ref} represents the calculated shielding constant of a reference carbon (the carbon of an allylic CH in **2**), σ_{sample} is that of the carbene carbon in the sample, and δ_{sample} denotes the shielding constant of the carbene carbon in the sample, $\delta_{ref\,(exp.)}$ is the experimentally observed chemical shift of the reference carbon. The calculated ^{13}C NMR shielding (σ) of the reference carbon (in THF) = 80.415 ppm, and $\delta_{ref\,(exp.)}$ is 100.0 ppm (referenced to TMS at 0 ppm). The molecular orbitals were visualized by the Avogadro 1.2.0 program.*(26)*

Table S8. Calculated chemical shielding values (in ppm) of IAd at the CPCM-wB97X-D3/def2-TZVP level in THF solution.

	σ_{total}	σ^{dia}	σ^{para}
σ_{iso}	-33.673	269.589	-303.261
σ_x	-9.068	277.906	-286.975
σ_y	144.418	254.925	-110.507
σ_z	-236.367	275.935	-512.302

Table S9. Calculated chemical shielding values (in ppm) of **2** at the CPCM-wB97X-D3/def2-TZVP level in THF solution.

	σ_{total}	σ^{dia}	σ^{para}
σ_{iso}	207.444	275.801	-68.356
σ_x	130.890	304.012	-173.122
σ_y	159.995	269.732	-109.736
σ_z	331.447	253.659	77.789

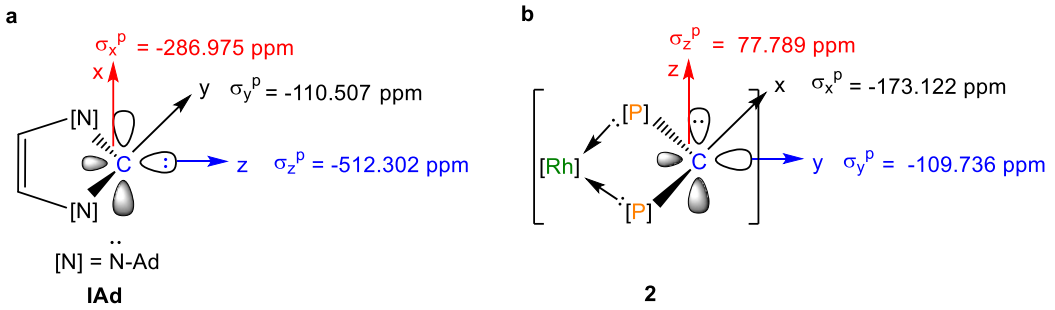

Fig. S37. Calculated chemical shielding values on the x, y, z axes of IAd (a) and **2** (b). The total paramagnetic shielding term (σ_x^p, σ_y^p and σ_z^p) along the respective x, y, z axes are given.

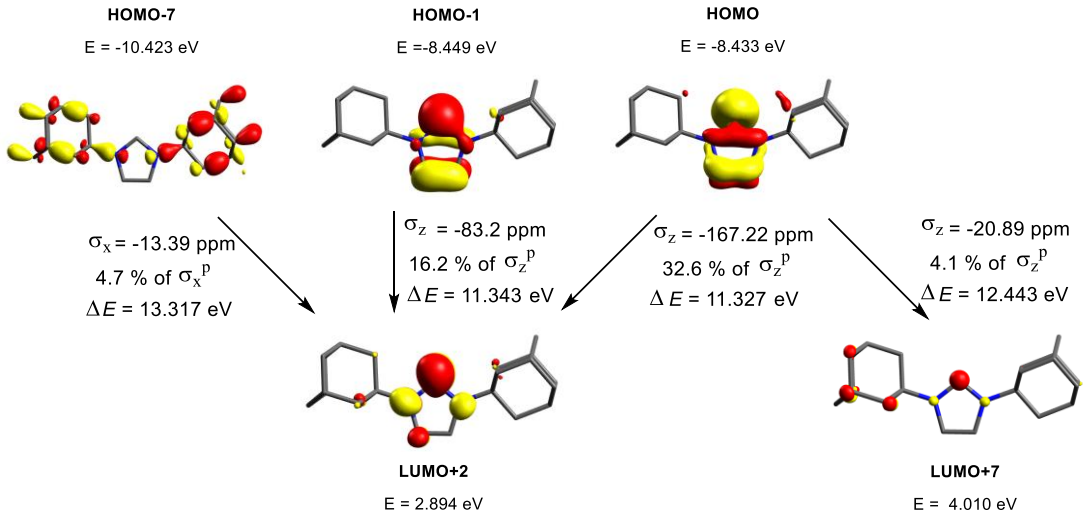

Fig. S38. Important magnetic couplings for the paramagnetic shielding term of IAd. For each coupling pathway, its contribution and percentage to the total paramagnetic shielding term (σ_x^p, σ_z^p), and the energy difference of the constituent canonical MOs are given.

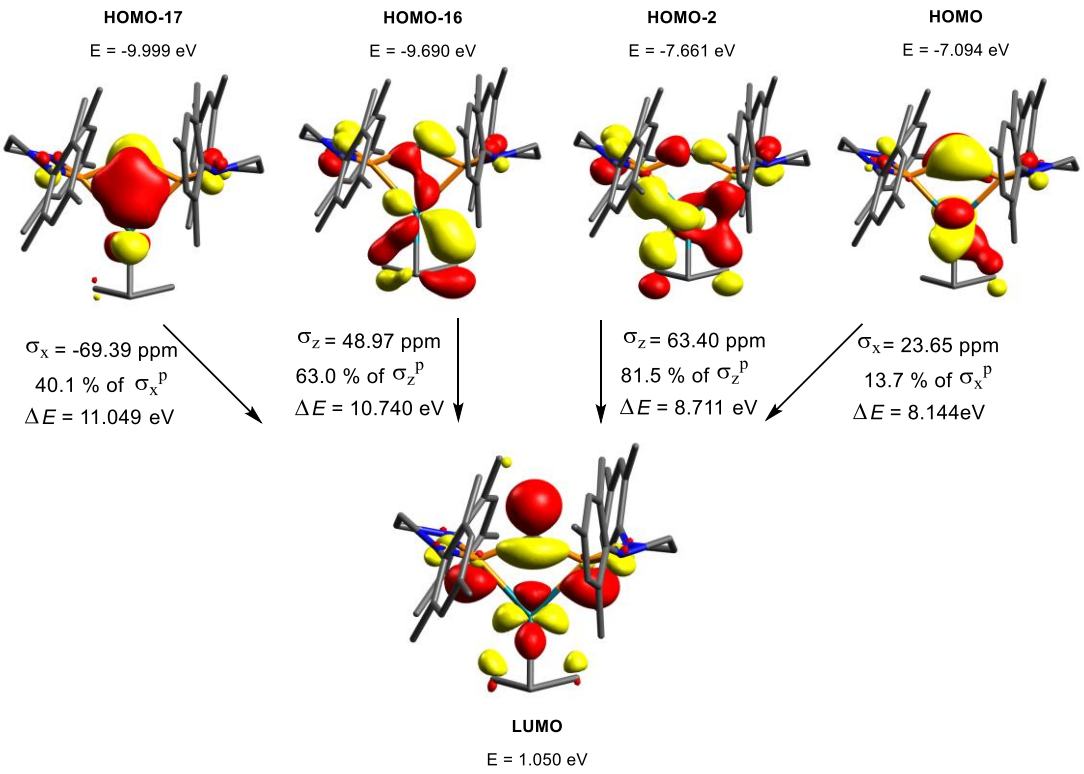

Fig. S39. Important magnetic couplings for the paramagnetic shielding term of complex **2**. For each coupling pathway, its contribution and percentage to the total paramagnetic shielding term (σ_x^p, σ_z^p), and the energy difference of the constituent canonical MOs are given.

8.4 Regarding the observed asynchronicity

We note that the steric and structural anisotropy associated with the allyl fragment can promote asynchronous H-H addition. To explicitly probe this effect, we constructed a model system (**2-acac**) in which the η^3-allyl is replaced by an acetylacetonate (acac) ligand, thereby rendering the regions above and below the carbene center nearly symmetric. Notably, even in this model system, the computed transition structure for H_2 addition remains distinctly asynchronous (Fig. S40).

Further analysis reveals that, upon geometry optimization, the pocket defined by the $[(CH_2)(NMes)]_2P$ substituents cannot achieve complete symmetry due to their intrinsic conformational flexibility in both **2** and **2-acac**. Even when the four Mes groups are replaced by hydrogen atoms, the pocket remains conformationally anisotropic. This intrinsic conformational asymmetry provides a natural origin for the observed asynchronicity.

To interrogate the origin of synchronicity versus asynchronicity more systematically, we modeled four cyclic diboryl carbenes (DBCs) featuring different substituents at boron and/or backbone modifications (Fig. S41). In the singlet state, all four systems adopt a $\sigma^0\pi^2$ electronic configuration. Importantly, the H/H, H/Mes, and Mes/Mes substituted DBCs possess high symmetry above and below the carbene center and exhibit nearly synchronous H-H addition. In contrast, backbone modification (replacement of two *syn*-H atoms by methyl groups) generates an asymmetric environment around the carbene center; modeling of this asymmetric DBC with H_2 indeed results in asynchronous H-H addition.

These results demonstrate that the observed asynchronicity in our system is not an intrinsic electronic feature of the $\sigma^0\pi^2$ carbene framework, but rather arises from steric and structural anisotropy in the approach pocket. As H_2 approaches the carbene center, the asymmetric pocket environment weakly polarizes the H-H bond and enforces a slightly slanted approach geometry in the transition region. This, in turn, enables preferential orbital interaction not only between $\sigma(H_2)$ and in-plane σ-accepting orbital but also one out-of-plane π-donating orbital of the carbene and one lobe of $\sigma^*(H_2)$, imparting partial heterolytic character and favoring unequal development of the two incipient C-H interactions. During geometry optimization, the system therefore converges to an asynchronous yet concerted transition state.

Consistent with this interpretation, constrained relaxed potential energy scans enforcing a strictly symmetric (synchronous) pathway—by fixing the two forming C-H distances to be equal—lead to a transition-state-like structure (**TS3**) at a C-H distance of 1.64 Å (Fig. S42). This structure represents a pseudo-transition state and corresponds to a higher-energy stationary point (0.86 kcal mol^{-1} above the true asynchronous **TS1**). **TS3** exhibits two imaginary frequencies: one associated with H-H bond cleavage (-899 cm^{-1}) and a second corresponding to the symmetry-breaking coordinate (-383 cm^{-1}). In contrast, unconstrained optimization initiated from **TS3** converges to the true first-order saddle point (**TS1**), characterized by a single dominant imaginary frequency and an intrinsically asynchronous pattern of bond formation.

We therefore conclude that the observed asynchronicity arises from inherent conformational asymmetry and steric/structural anisotropy of the reactive pocket. The hydrogenation proceeds via a concerted σ-face pathway, in which minimal atom reorganization is maintained, while subtle geometric anisotropy naturally leads to asynchronous C-H bond formation.

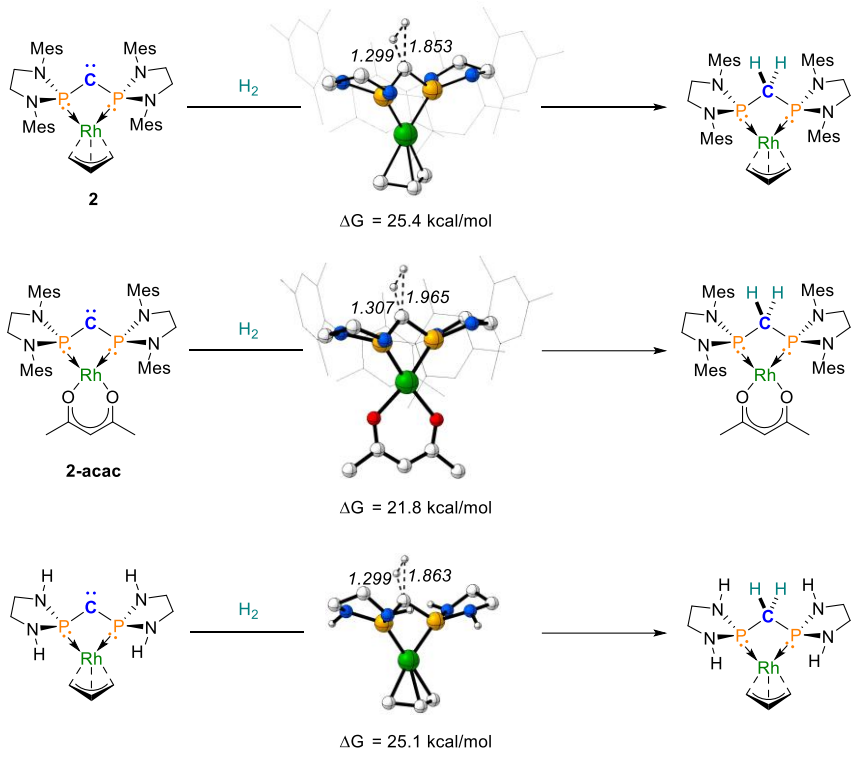

Fig. S40. Comparison of the effects of allyl/acac ligands and mesityl-to-hydrogen substitution on H-H addition synchronicity. *Notably, the computed transition structure for H_2 addition remains distinctly asynchronous.*

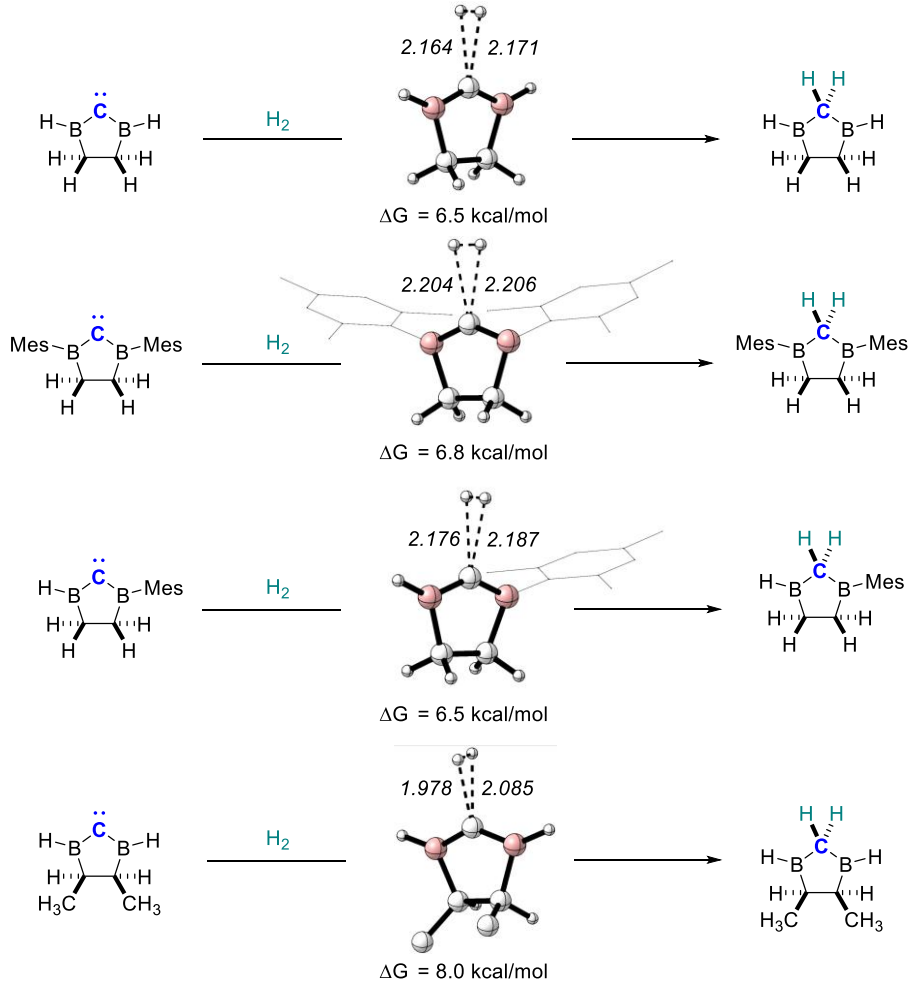

Fig. S41. Substituent/backbone modification effects on H-H addition synchronicity of cyclic diboryl carbenes. *Symmetric DBCs (H/H, H/Mes, Mes/Mes): nearly synchronous H-H addition; Methyl-substituted asymmetric DBC: asynchronous H-H addition.*

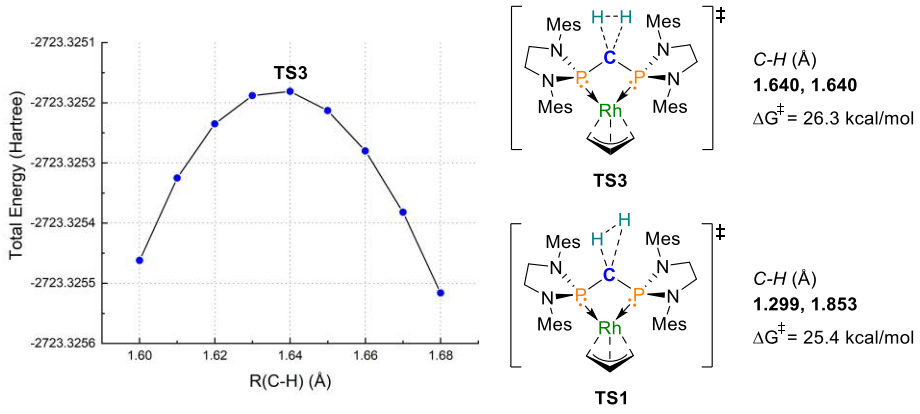

Fig. S42. Relaxed potential energy scan for C-H bond formation: synchronous pseudo-TS (**TS3**, 1.640 Å, 26.3 kcal mol^{-1}) *vs*. asynchronous true TS (**TS1**, 1.299/1.853 Å, 25.4 kcal mol^{-1}).

8.5 IBO calculations for **2**.

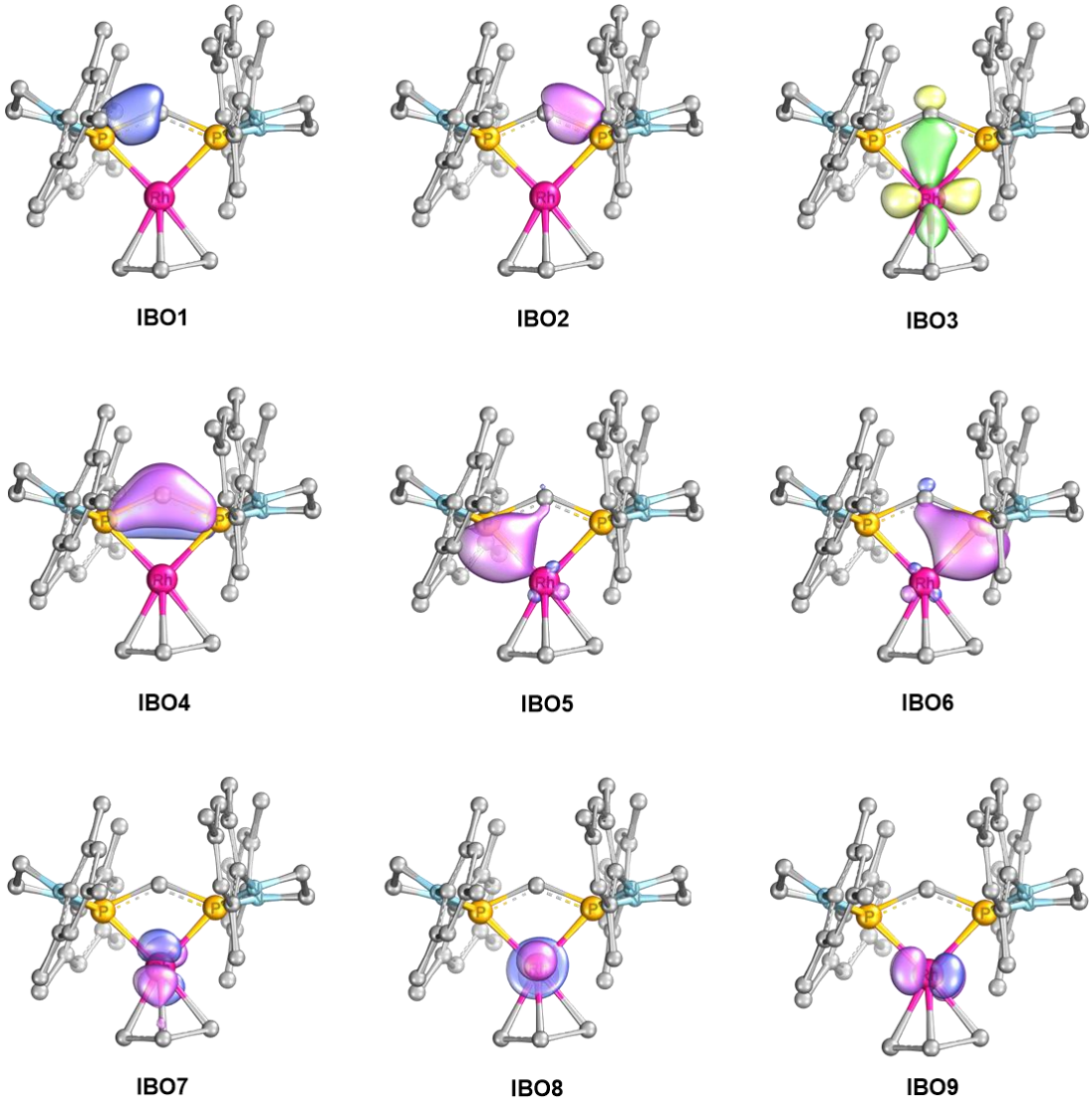

Fig. S43. Depiction of selected IBOs of **2**. (**IBO1**) P(1)–C(1) σ-bonding orbital. (**IBO2**) P(2)–C(1) σ- bonding orbital. (**IBO3**) σ donation (in-plane) from the Rh center. (**IBO4**) C(1) lone pair orbital. (**IBO5**) P(1)–Rh(1) σ-bonding orbital. (**IBO6**) P(2)–Rh(1) σ-bonding orbital. (**IBO7, IBO8 and IBO9**) Rh(1) nonbonding d-orbitals (lone-pair orbitals). Threshold value = 73%.

8.6 FMOs calculations for cationic $\sigma^0\pi^2$ carbene **A**.

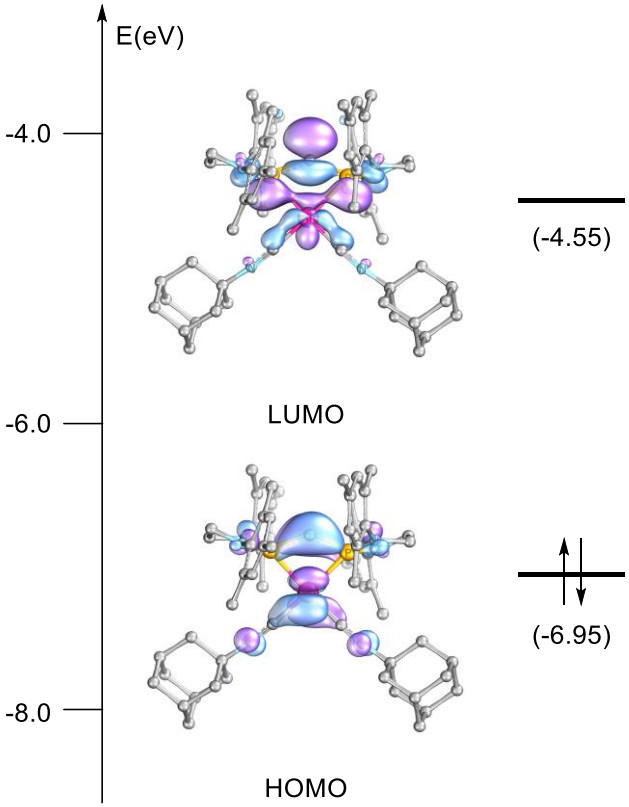

Fig. S44. Energy diagram for the frontier Kohn-Sham orbitals. Threshold value = 73%.

8.7 Gibbs free energy profiles for H_2 activation by **2** and **CAAC** (kcal/mol).

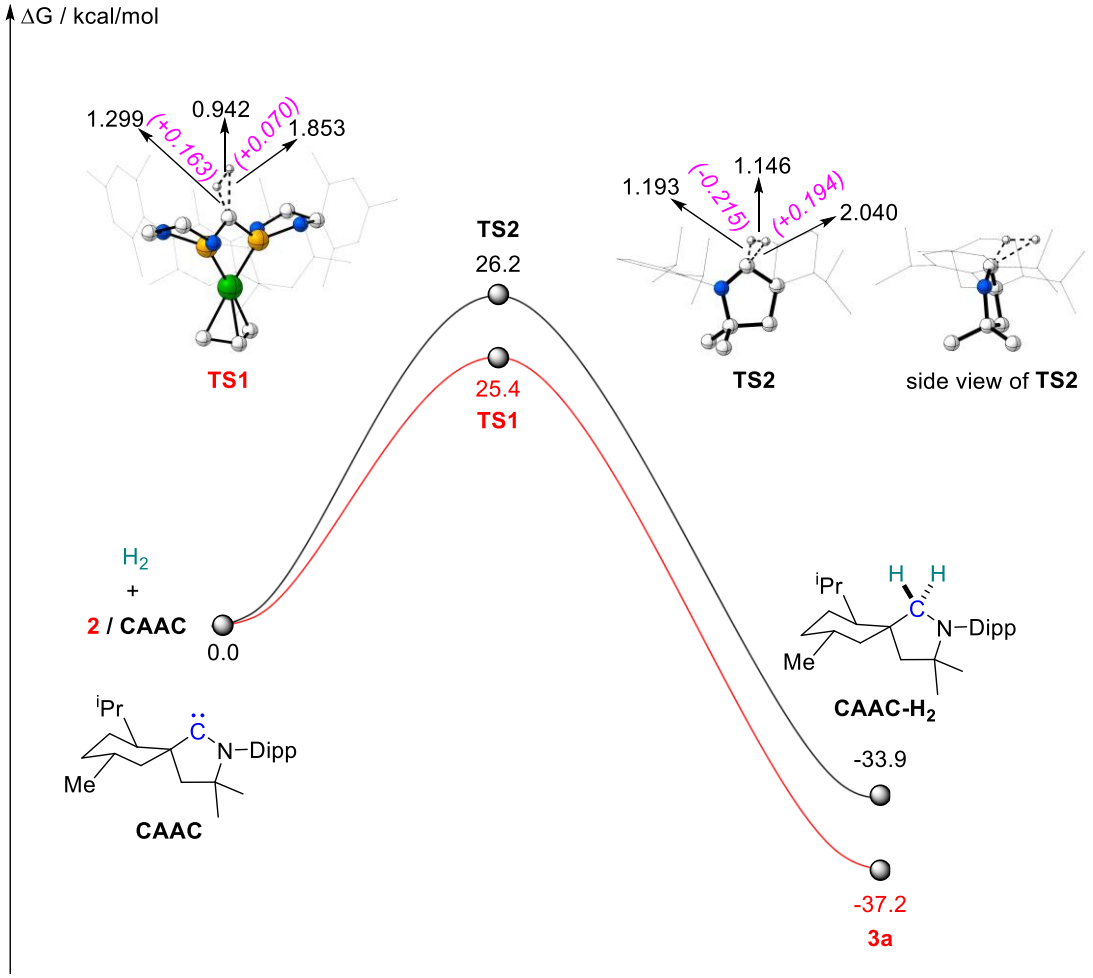

Fig. S45. DFT-calculated free-energy profile (kcal/mol) for H_2 activation by **2** (red) and **CAAC** (black). Selected bond lengths (Å) and NPA charges (a.u., in parentheses) of the two hydrogen atoms (**TS1** and **TS2**).

Table S10. Enthalpy (ΔH) and entropy (ΔS) changes for the hydrogenation of **2**.

	2+H_2	**TS1**	**3a**
ΔH (kcal/mol)	0.0	17.0	-47.3
ΔS kcal/(mol·K)	0.0	-28.2	-34.0

Table S11. Enthalpy (ΔH) and entropy (ΔS) changes for the hydrogenation of **CAAC**.

	CAAC+H_2	**TS2**	**CAAC-H₂**
ΔH (kcal/mol)	0.0	17.1	-42.5
ΔS kcal/(mol·K)	0.0	-30.7	-28.9

8.8 Heavy-atom root-mean-square deviation (RMSD) of **2** and **CAAC**.

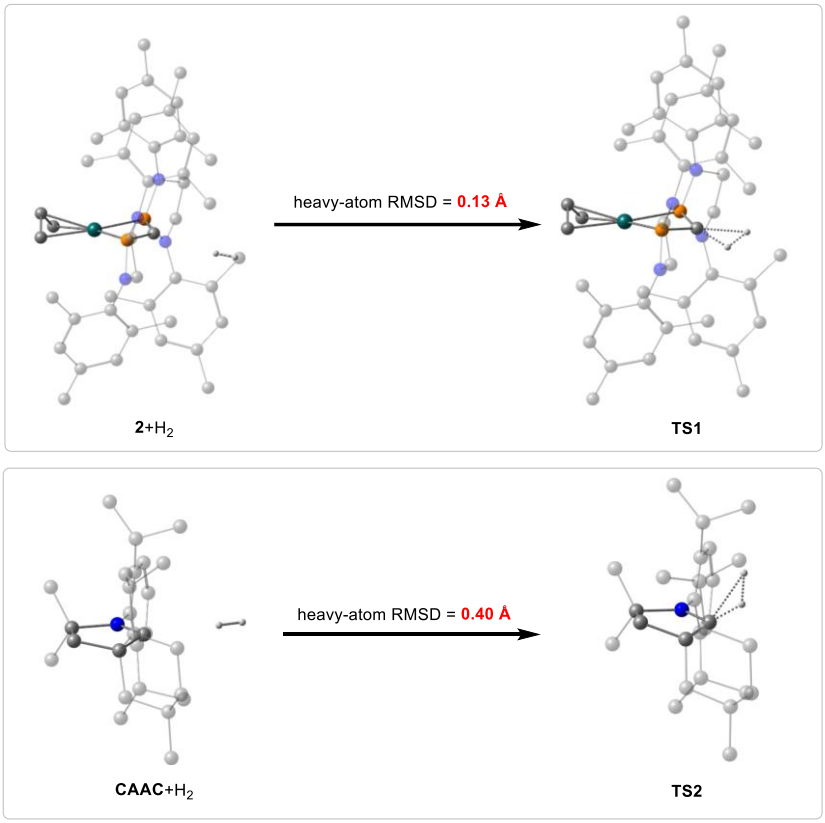

Fig. S46. Comparative RMSD of **2** (above) and **CAAC** (below). Heavy-atom = any atom except H.

8.9 Activation strain model (ASM) analysis of **2** and **CAAC**.

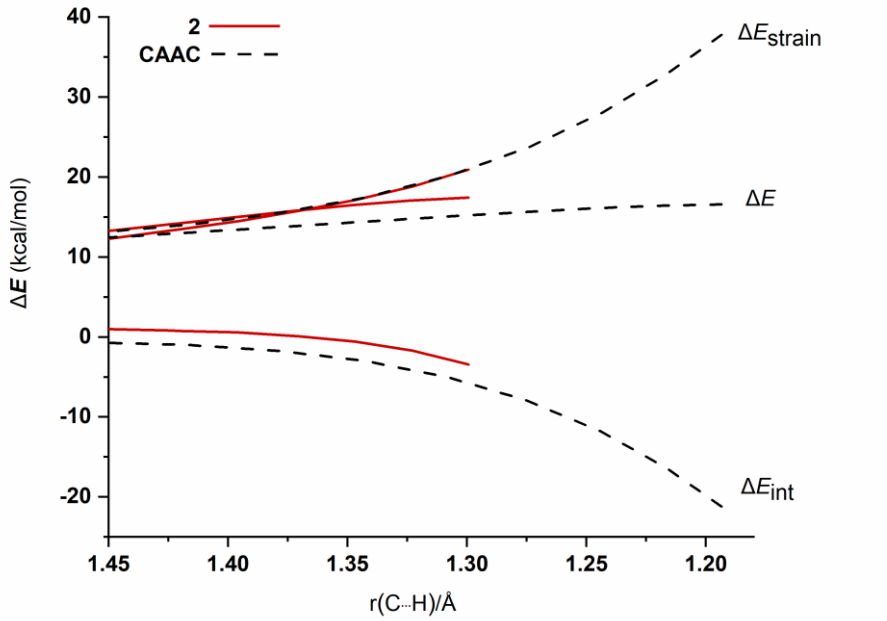

Fig. S47. Comparative ASM analyses for the reactions of H_2 with **2** (red) and **CAAC** (black) projected onto the C···H bond-forming distance.

Table S12. ASM analysis of **2** and **CAAC**.

	(**2**+H_2) →**TS1**	(**CAAC**+H_2)→**TS2**
ΔE_{strain} (kcal/mol)	20.91	37.78
ΔE_{int} (kcal/mol)	-3.46	-21.22
ΔE (kcal/mol)	17.44	16.56

8.10 NLMOs of **TS1** and **TS2**.

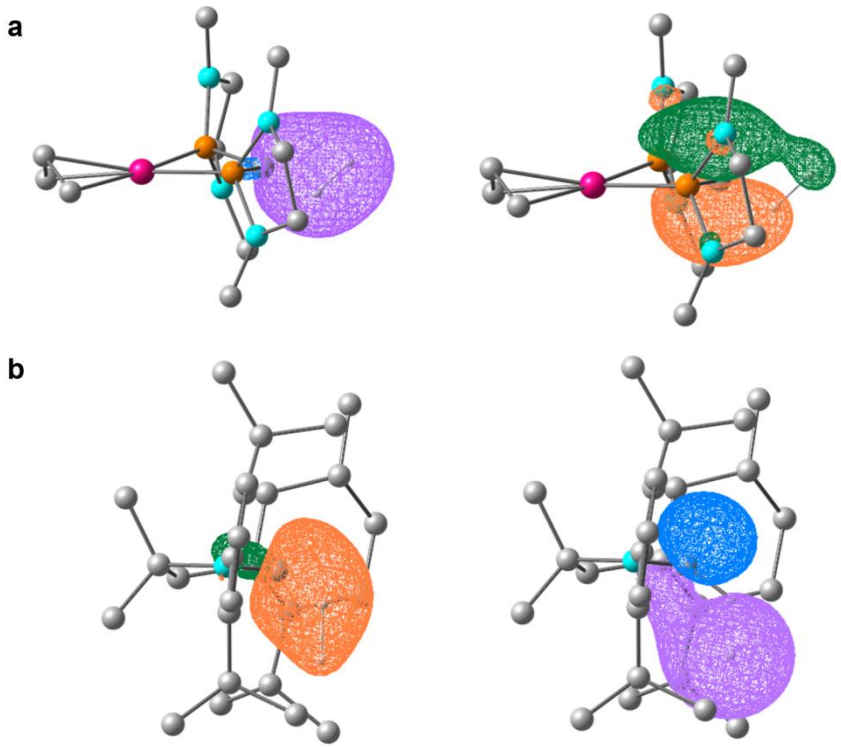

Fig. S48. NLMOs analysis. **a**, Selected NLMOs for **TS1**. **b**, Selected NLMOs for **TS2**.

8.11 2D deformation density and ELF maps.

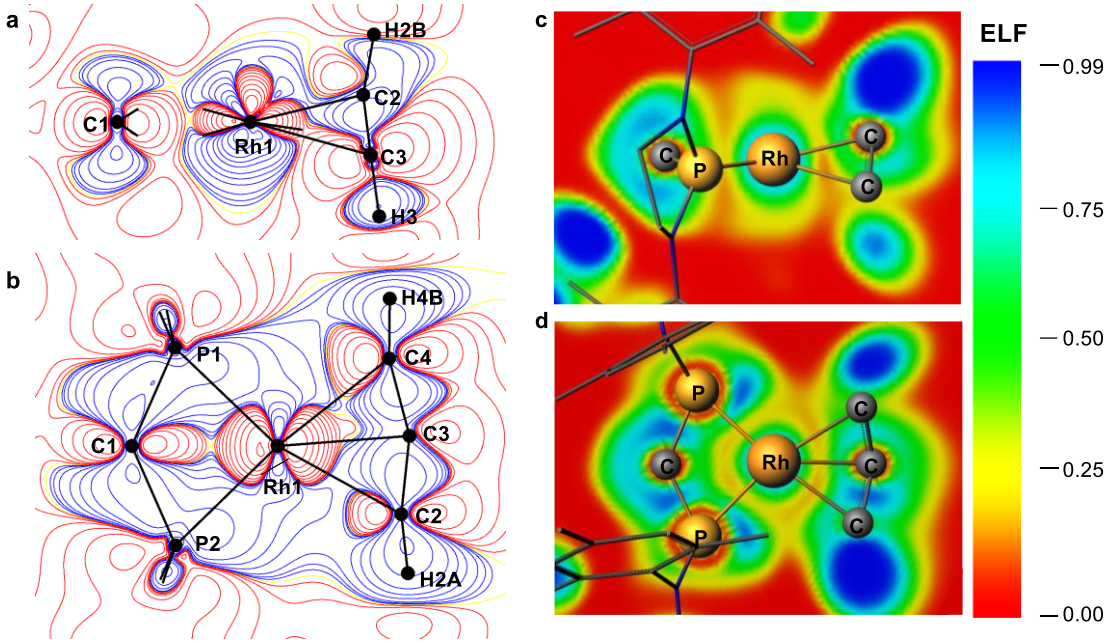

Fig. S49. Comparison of 2D deformation density (a, b) and ELF (c, d) maps for **2**. **a** and **b**, Contours are at 0.05 e Å^{-3} level. Blue = positive deformation density (*e.g.* in bonds or lone pairs), red = negative deformation density. **c** and **d**, Viewed from top and side, respectively.

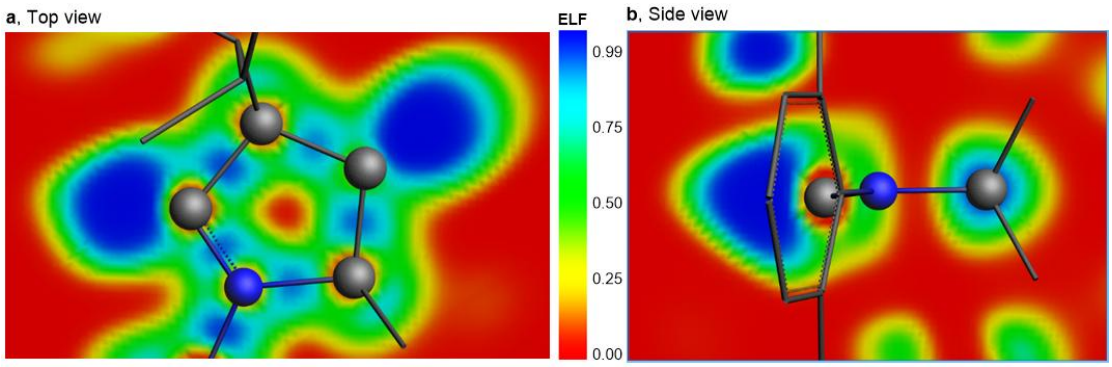

Fig. S50. ELF analysis of **CAAC**, viewed from top and side, respectively.

Cartesian Coordinates

2 (singlet)

45	0.001235000	-0.644309000	1.611425000
15	0.011948000	-1.516014000	-0.443304000
15	-0.019893000	1.384373000	0.662568000
7	1.218137000	2.563887000	0.729906000
7	1.242641000	-2.316423000	-1.328068000
7	-1.204720000	-2.404010000	-1.262452000
7	-1.250910000	2.588331000	0.694072000
6	2.566551000	2.386087000	0.291029000
6	2.626824000	-2.114374000	-1.035412000
6	2.961642000	2.988902000	-0.933790000
6	3.322880000	-1.094199000	-1.731444000
6	-2.591093000	-2.147125000	-1.028252000
6	-2.935173000	2.648563000	-1.111924000
6	-2.585139000	2.347653000	0.232701000
6	3.502725000	1.658764000	1.067273000
6	3.283668000	-2.915541000	-0.067248000
6	4.694792000	-0.924388000	-1.474437000
1	5.241857000	-0.146378000	-2.028526000
6	0.045717000	0.193884000	-0.523904000
6	4.309747000	2.915112000	-1.324821000
1	4.615118000	3.391174000	-2.272126000
6	4.653633000	-2.696142000	0.169347000
1	5.168604000	-3.315297000	0.923538000
6	-3.296457000	-1.206531000	-1.818748000
6	-3.238464000	-2.842551000	0.024212000
6	5.379536000	-1.713423000	-0.531063000
6	5.272882000	2.247766000	-0.542368000
6	4.841878000	1.610249000	0.633457000
1	5.572212000	1.057690000	1.246512000
6	-0.701173000	-3.122726000	-2.434783000
1	-0.728178000	-2.495242000	-3.358454000
1	-1.309169000	-4.032945000	-2.617343000
6	1.944300000	3.680779000	-1.805720000
1	1.019562000	3.075119000	-1.883260000
1	2.342038000	3.850617000	-2.825238000
1	1.642252000	4.671127000	-1.399800000
6	-4.601809000	-2.591797000	0.260235000
1	-5.109106000	-3.134031000	1.076052000
6	-4.897227000	1.756939000	0.695095000
1	-5.658821000	1.390330000	1.403074000
6	-3.560376000	1.846274000	1.129819000

6	-5.288086000	2.141141000	-0.599359000
6	-5.335868000	-1.682456000	-0.525972000
6	0.751798000	-3.474652000	-2.075346000
1	0.784982000	-4.415642000	-1.474047000
1	1.369459000	-3.627971000	-2.985285000
6	-4.284352000	2.556359000	-1.495996000
1	-4.557449000	2.809997000	-2.534679000
6	0.722000000	3.834352000	1.257916000
1	1.345608000	4.672305000	0.886332000
1	0.766069000	3.853692000	2.373440000
6	-4.664907000	-1.004307000	-1.560335000
1	-5.216759000	-0.281036000	-2.180689000
6	-2.467483000	-3.823309000	0.869540000
1	-1.919687000	-4.557495000	0.243467000
1	-3.134930000	-4.372496000	1.562049000
1	-1.699349000	-3.290421000	1.466700000
6	-2.590963000	-0.432435000	-2.903549000
1	-1.623350000	-0.039262000	-2.528264000
1	-3.208524000	0.422362000	-3.238937000
1	-2.376277000	-1.063735000	-3.793412000
6	-1.881145000	3.022143000	-2.124114000
1	-1.540502000	4.075385000	-2.020795000
1	-2.265052000	2.902761000	-3.155856000
1	-0.988570000	2.372967000	-2.009535000
6	-0.734333000	3.958435000	0.768624000
1	-1.345063000	4.563587000	1.471933000
1	-0.762667000	4.462437000	-0.225111000
6	2.597038000	-0.211188000	-2.713131000
1	2.066664000	-0.807204000	-3.484970000
1	3.293378000	0.490125000	-3.212044000
1	1.820619000	0.379804000	-2.179567000
6	6.719121000	2.203729000	-0.976785000
1	6.839065000	1.653358000	-1.935588000
1	7.356839000	1.702825000	-0.222605000
1	7.123289000	3.224594000	-1.143524000
6	6.845958000	-1.488602000	-0.245746000
1	7.356422000	-0.993104000	-1.095363000
1	7.373127000	-2.440823000	-0.031961000
1	6.984273000	-0.835482000	0.644407000
6	3.075118000	0.940483000	2.314926000
1	2.475120000	1.597810000	2.976649000
1	3.945238000	0.554501000	2.880344000
1	2.407677000	0.080607000	2.055173000
6	-0.055153000	-0.008008000	3.726257000

1	0.994846000	0.113451000	4.039683000
1	-0.732585000	0.806806000	4.023785000
6	0.299665000	-2.308152000	3.000663000
1	-0.097613000	-3.307229000	2.760272000
1	1.375502000	-2.280921000	3.247558000
6	2.527998000	-3.980675000	0.688272000
1	1.508297000	-3.631816000	0.945733000
1	3.050238000	-4.251614000	1.626892000
1	2.421111000	-4.911817000	0.089440000
6	-3.164894000	1.396568000	2.509697000
1	-2.590645000	0.446186000	2.437441000
1	-4.049633000	1.229502000	3.154085000
1	-2.489983000	2.130352000	2.994953000
6	-6.734516000	2.104681000	-1.032578000
1	-7.395026000	1.730141000	-0.226607000
1	-6.879126000	1.450102000	-1.918794000
1	-7.091660000	3.116177000	-1.321820000
6	-0.583183000	-1.322426000	3.537466000
1	-1.662143000	-1.530168000	3.653453000
6	-6.795062000	-1.422217000	-0.236785000
1	-7.311404000	-2.338318000	0.115963000
1	-7.330541000	-1.045208000	-1.130560000
1	-6.909765000	-0.656013000	0.561029000

2 (triplet)

45	-0.031965000	0.070494000	1.887207000
15	0.019971000	-1.413110000	0.179316000
15	-0.047081000	1.408309000	0.068096000
7	1.216477000	-2.565506000	-0.289831000
7	-1.229023000	-2.563706000	-0.136725000
7	-1.247421000	2.494515000	-0.528504000
7	1.187707000	2.577276000	-0.257981000
6	0.046684000	-0.042201000	-0.970137000
6	-3.360572000	-1.722322000	-1.069514000
6	-2.611649000	-2.237953000	0.018356000
6	2.546821000	-2.239811000	-0.693283000
6	-3.222019000	-2.469911000	1.277691000
6	3.545867000	-1.980538000	0.278879000
6	-4.735440000	-1.485326000	-0.881358000
1	-5.323279000	-1.101132000	-1.729264000
6	2.871835000	-2.231188000	-2.076495000
6	-2.599793000	2.148765000	-0.814560000
6	-0.747550000	3.853208000	-0.755311000
1	-0.878604000	4.486947000	0.155243000

1	-1.306396000	4.338754000	-1.581263000
6	-3.526679000	1.892521000	0.227797000
6	-2.703462000	-1.428238000	-2.394378000
1	-1.746563000	-0.879415000	-2.242183000
1	-3.361837000	-0.804904000	-3.028866000
1	-2.465034000	-2.357494000	-2.956712000
6	-4.590048000	-2.181845000	1.428275000
1	-5.067406000	-2.362405000	2.406379000
6	-1.997794000	2.226806000	-3.281514000
1	-1.676047000	3.278519000	-3.448056000
1	-2.408327000	1.855367000	-4.241015000
1	-1.085105000	1.645202000	-3.034079000
6	-2.412222000	-3.054178000	2.407250000
1	-2.093902000	-4.093280000	2.174581000
1	-2.993001000	-3.076178000	3.350413000
1	-1.484477000	-2.470044000	2.569656000
6	0.738423000	3.691722000	-1.094071000
1	0.865315000	3.483314000	-2.184026000
1	1.320353000	4.605705000	-0.850537000
6	-5.368436000	-1.702405000	0.355672000
6	3.180767000	-1.869104000	1.733360000
1	2.599420000	-0.934816000	1.903579000
1	4.080100000	-1.848111000	2.378858000
1	2.519588000	-2.700859000	2.050639000
6	2.577524000	2.258298000	-0.128161000
6	1.790614000	-2.376030000	-3.118825000
1	1.433131000	-3.424135000	-3.219771000
1	2.156300000	-2.057777000	-4.114796000
1	0.910112000	-1.754821000	-2.850300000
6	0.674818000	-3.914675000	-0.493421000
1	0.731905000	-4.513997000	0.446537000
1	1.263431000	-4.448349000	-1.266878000
6	-3.014510000	2.101002000	-2.173675000
6	4.875983000	-1.813465000	-0.147952000
1	5.655146000	-1.644564000	0.613563000
6	-0.786923000	-3.719608000	-0.916317000
1	-0.855083000	-3.545826000	-2.017410000
1	-1.413212000	-4.602763000	-0.669587000
6	3.278210000	1.637412000	-1.200934000
6	4.215935000	-2.059004000	-2.455662000
1	4.469444000	-2.067363000	-3.529532000
6	5.239177000	-1.874042000	-1.505600000
6	-4.376053000	1.900628000	-2.460770000
1	-4.698919000	1.875546000	-3.515688000

6	2.577902000	1.266519000	-2.482825000
1	1.649992000	0.685821000	-2.266911000
1	3.232849000	0.644229000	-3.121586000
1	2.275498000	2.162072000	-3.067672000
6	-4.878927000	1.693122000	-0.109674000
1	-5.603027000	1.517141000	0.702305000
6	-3.074532000	1.814162000	1.660098000
1	-2.485369000	0.877363000	1.826021000
1	-3.933670000	1.808524000	2.358591000
1	-2.391888000	2.646944000	1.923576000
6	-0.003970000	1.419314000	3.636495000
1	-1.066665000	1.335900000	3.930822000
1	0.396728000	2.440824000	3.594268000
6	0.336812000	-1.008162000	3.783803000
1	-0.695095000	-1.189954000	4.135254000
1	1.012817000	-1.874700000	3.836639000
6	-5.331316000	1.721928000	-1.440195000
6	-6.837022000	-1.404060000	0.545052000
1	-6.984348000	-0.432351000	1.066207000
1	-7.335117000	-2.178916000	1.163676000
1	-7.369923000	-1.339976000	-0.424094000
6	6.674965000	-1.694959000	-1.939875000
1	6.873228000	-0.648347000	-2.262018000
1	6.927111000	-2.349626000	-2.799059000
1	7.381598000	-1.919521000	-1.115918000
6	4.649448000	1.376408000	-1.046586000
1	5.190218000	0.909882000	-1.884324000
6	3.254549000	2.594570000	1.070857000
6	2.558338000	3.332899000	2.186209000
1	2.968134000	4.360601000	2.292696000
1	2.706797000	2.825550000	3.161617000
1	1.474362000	3.407573000	1.987762000
6	-6.791358000	1.532039000	-1.778722000
1	-7.172369000	2.361426000	-2.411326000
1	-7.418635000	1.481931000	-0.867311000
1	-6.957460000	0.592960000	-2.350897000
6	5.342694000	1.681930000	0.141518000
6	4.624818000	2.283311000	1.188400000
1	5.150071000	2.544557000	2.122933000
6	6.809240000	1.352919000	0.286357000
1	7.367750000	1.557322000	-0.650203000
1	6.954383000	0.274952000	0.516640000
1	7.281517000	1.932920000	1.104282000
6	0.861929000	0.314963000	3.857805000

1	1.955900000	0.472977000	3.859987000

TS1

45	3.560289000	7.823858000	7.306750000
15	4.732753000	6.393308000	6.040961000
15	5.529106000	8.907878000	7.300228000
7	5.167648000	4.744561000	6.339382000
7	4.490272000	6.048343000	4.368966000
7	6.137845000	10.300714000	6.493806000
7	6.321707000	9.379286000	8.751311000
6	6.074194000	7.407920000	6.566952000
1	7.276205000	6.952315000	6.755848000
1	7.834083000	7.181176000	6.032410000
6	5.290239000	7.577325000	2.600403000
6	4.228766000	7.045707000	3.376658000
6	5.944024000	4.318697000	7.454777000
6	2.886497000	7.428153000	3.118702000
6	5.391084000	4.330408000	8.765352000
6	4.975967000	8.429951000	1.524727000
1	5.799541000	8.822484000	0.907273000
6	7.288016000	3.893887000	7.252752000
6	6.068788000	10.560292000	5.092643000
6	6.609153000	11.334277000	7.420506000
1	5.782123000	12.020190000	7.728194000
1	7.387780000	11.954778000	6.930841000
6	4.839059000	10.881772000	4.463543000
6	6.729245000	7.240075000	2.901700000
1	6.894099000	7.155927000	3.994495000
1	7.400820000	8.031997000	2.517087000
1	7.040869000	6.278229000	2.437207000
6	2.625690000	8.311661000	2.057203000
1	1.580531000	8.598551000	1.851355000
6	8.570383000	10.119743000	5.000415000
1	8.924342000	10.828166000	5.780413000
1	9.379042000	10.020820000	4.249919000
1	8.434756000	9.137677000	5.504194000
6	1.768991000	6.881139000	3.964493000
1	1.821119000	5.775076000	4.038599000
1	0.777304000	7.169559000	3.564967000
1	1.865390000	7.260922000	5.001884000
6	7.163673000	10.569713000	8.632621000
1	8.235093000	10.297561000	8.469328000
1	7.107983000	11.176692000	9.559729000
6	3.653667000	8.803081000	1.228976000

6	4.005163000	4.849914000	9.013216000
1	3.985534000	5.966138000	8.906761000
1	3.651193000	4.593678000	10.030545000
1	3.284775000	4.467815000	8.262470000
6	5.994132000	8.753544000	9.991736000
6	7.924936000	3.939931000	5.885305000
1	7.653216000	3.060024000	5.261644000
1	9.029583000	3.954417000	5.963971000
1	7.603628000	4.841135000	5.324625000
6	4.802114000	3.856932000	5.235111000
1	3.757278000	3.480761000	5.352440000
1	5.471692000	2.974659000	5.208360000
6	7.282708000	10.566093000	4.354837000
6	6.181641000	3.878938000	9.838387000
1	5.739389000	3.876757000	10.847992000
6	4.926034000	4.707449000	3.964453000
1	5.977983000	4.699308000	3.590464000
1	4.271513000	4.329933000	3.150988000
6	6.643230000	7.550025000	10.364197000
6	8.038177000	3.454219000	8.360552000
1	9.081421000	3.134235000	8.199326000
6	7.504810000	3.434923000	9.662690000
6	7.257417000	10.986823000	3.013291000
1	8.203359000	11.012713000	2.445789000
6	7.753226000	6.968446000	9.527708000
1	7.347955000	6.253554000	8.782939000
1	8.473971000	6.410423000	10.156807000
1	8.295839000	7.754984000	8.968565000
6	4.865135000	11.295370000	3.117688000
1	3.913871000	11.571615000	2.634857000
6	3.538980000	10.790960000	5.216792000
1	3.325546000	9.732515000	5.505836000
1	2.695124000	11.169990000	4.608673000
1	3.576072000	11.358071000	6.170635000
6	1.547211000	6.926592000	7.571696000
1	1.666686000	6.419647000	8.544258000
1	1.065851000	6.328561000	6.782848000
6	2.210151000	9.122154000	8.464662000
1	2.371850000	8.744988000	9.489883000
1	2.236064000	10.216170000	8.348469000
6	6.061756000	11.386194000	2.384536000
6	3.333453000	9.726266000	0.077445000
1	3.110019000	10.755047000	0.435970000
1	2.439900000	9.381183000	-0.482933000

1	4.178482000	9.802736000	-0.634701000
6	8.343170000	3.012755000	10.846332000
1	8.830514000	3.892796000	11.322966000
1	9.151007000	2.313230000	10.551203000
1	7.728314000	2.521383000	11.627808000
6	6.230758000	6.901063000	11.544741000
1	6.737962000	5.967937000	11.838408000
6	4.990688000	9.322995000	10.821424000
6	4.375959000	10.655426000	10.473536000
1	5.023547000	11.495486000	10.809439000
1	3.389589000	10.786462000	10.959369000
1	4.246434000	10.758679000	9.379283000
6	6.076598000	11.877191000	0.956194000
1	6.859659000	12.648905000	0.802510000
1	5.102351000	12.315109000	0.663771000
1	6.296430000	11.051992000	0.244175000
6	5.199408000	7.409970000	12.354074000
6	4.603575000	8.633196000	11.983814000
1	3.810831000	9.063024000	12.619331000
6	4.728181000	6.659252000	13.578102000
1	5.494725000	5.944480000	13.939290000
1	3.809522000	6.072893000	13.354810000
1	4.477027000	7.347235000	14.411408000
6	1.471504000	8.345568000	7.526988000
1	1.019450000	8.840731000	6.647605000

3a

45	0.164379000	-0.802329000	1.592735000
15	0.162677000	-1.095357000	-0.633305000
15	-0.039460000	1.235275000	0.718038000
7	1.107479000	2.513302000	1.011443000
7	1.349656000	-1.844091000	-1.666775000
7	-1.112478000	-1.803680000	-1.567643000
7	-1.359217000	2.354373000	0.892729000
6	2.413351000	2.559652000	0.448773000
6	2.698400000	-1.984323000	-1.212531000
6	2.696501000	3.481321000	-0.601362000
6	3.673557000	-1.046047000	-1.636680000
6	-2.499146000	-1.783609000	-1.226095000
6	-3.225415000	2.697485000	-0.688419000
6	-2.700372000	2.078504000	0.481332000
6	3.427288000	1.669296000	0.900309000
6	3.056047000	-3.038904000	-0.325865000
6	4.987300000	-1.159770000	-1.138465000

1	5.746143000	-0.436674000	-1.479119000
6	0.221687000	0.747845000	-1.061789000
6	3.991494000	3.519523000	-1.150525000
1	4.199605000	4.230842000	-1.967649000
6	4.371339000	-3.094880000	0.165989000
1	4.640953000	-3.901230000	0.869081000
6	-3.417354000	-0.972663000	-1.943208000
6	-2.968244000	-2.653199000	-0.202311000
6	5.351792000	-2.157058000	-0.219006000
6	5.013825000	2.656663000	-0.708011000
6	4.705599000	1.742512000	0.314063000
1	5.485548000	1.055756000	0.678708000
6	-0.643239000	-2.184353000	-2.904299000
1	-0.605376000	-1.319799000	-3.611410000
1	-1.320913000	-2.950317000	-3.333744000
6	1.616169000	4.377413000	-1.153018000
1	0.659593000	3.824958000	-1.248206000
1	1.895718000	4.772909000	-2.148918000
1	1.412252000	5.251761000	-0.497356000
6	-4.341359000	-2.674663000	0.096123000
1	-4.696952000	-3.352066000	0.890923000
6	-4.891138000	1.109074000	0.920727000
1	-5.535778000	0.476537000	1.552460000
6	-3.534938000	1.240179000	1.271831000
6	-5.451050000	1.775819000	-0.183029000
6	-5.274652000	-1.898869000	-0.617889000
6	0.773361000	-2.728341000	-2.680598000
1	0.731921000	-3.792580000	-2.344272000
1	1.373091000	-2.689368000	-3.616363000
6	-4.591847000	2.544949000	-0.988378000
1	-4.995129000	3.046750000	-1.884873000
6	0.488540000	3.610074000	1.754176000
1	1.059674000	4.547692000	1.603447000
1	0.481677000	3.396690000	2.850377000
6	-4.788762000	-1.063795000	-1.637126000
1	-5.496001000	-0.442356000	-2.209392000
6	-2.014830000	-3.563023000	0.521244000
1	-1.403557000	-4.150739000	-0.195429000
1	-2.552128000	-4.261308000	1.192130000
1	-1.295512000	-2.964710000	1.121580000
6	-2.966634000	-0.031257000	-3.033069000
1	-2.001580000	0.446530000	-2.778565000
1	-3.713424000	0.771666000	-3.185441000
1	-2.825247000	-0.551392000	-4.005758000

6	-2.354066000	3.510261000	-1.615781000
1	-2.310423000	4.582760000	-1.323641000
1	-2.741744000	3.471871000	-2.653196000
1	-1.311592000	3.135522000	-1.621823000
6	-0.949842000	3.725744000	1.222545000
1	-1.634105000	4.146807000	1.990262000
1	-0.976252000	4.402752000	0.338078000
6	3.338663000	0.064413000	-2.600528000
1	2.381599000	-0.130253000	-3.119746000
1	4.142202000	0.190832000	-3.354581000
1	3.251120000	1.036052000	-2.067880000
6	6.378102000	2.669623000	-1.355968000
1	6.368988000	2.099926000	-2.312050000
1	7.143469000	2.203582000	-0.703588000
1	6.710901000	3.699785000	-1.598265000
6	6.746062000	-2.210728000	0.361084000
1	7.472307000	-1.658612000	-0.268733000
1	7.106581000	-3.254268000	0.470473000
1	6.772919000	-1.752792000	1.374818000
6	3.149198000	0.659837000	1.974004000
1	2.710908000	1.140142000	2.872764000
1	4.064787000	0.107536000	2.259894000
1	2.379466000	-0.091389000	1.635516000
6	0.208776000	-0.450122000	3.777952000
1	1.263477000	-0.167210000	3.934693000
1	-0.530176000	0.199767000	4.270838000
6	0.707960000	-2.649188000	2.737046000
1	0.361496000	-3.662065000	2.483990000
1	1.804040000	-2.511303000	2.744905000
6	2.053907000	-4.100447000	0.052296000
1	1.046660000	-3.667475000	0.201525000
1	2.350723000	-4.616743000	0.985566000
1	1.974604000	-4.874292000	-0.742581000
6	-2.986048000	0.515164000	2.466125000
1	-2.270946000	-0.279563000	2.136369000
1	-3.792425000	0.050250000	3.065524000
1	-2.390793000	1.195447000	3.109036000
6	-6.919655000	1.659957000	-0.515439000
1	-7.484678000	1.163927000	0.297848000
1	-7.081725000	1.065684000	-1.441062000
1	-7.375193000	2.657023000	-0.690851000
6	-0.125878000	-1.808623000	3.519554000
1	-1.167170000	-2.135378000	3.702141000
6	-6.744486000	-1.954455000	-0.276273000

1	-7.076004000	-2.993394000	-0.070791000
1	-7.372016000	-1.547804000	-1.093929000
1	-6.967136000	-1.359383000	0.636685000
1	1.235505000	1.052424000	-1.396506000
1	-0.527121000	1.115029000	-1.793338000

CAAC (singlet)

7	0.507477000	-0.030094000	0.454187000
6	-0.555208000	0.077912000	-0.318863000
6	-1.760370000	0.122612000	0.612244000
6	-1.238191000	-0.235795000	2.042334000
1	-1.643561000	0.456527000	2.807083000
1	-1.556093000	-1.255271000	2.335874000
6	0.303013000	-0.160412000	1.983466000
6	-2.245934000	1.607704000	0.613116000
1	-3.015749000	1.701715000	1.414801000
1	-1.403091000	2.266941000	0.916516000
6	-2.845466000	2.102493000	-0.709754000
1	-2.054271000	2.013971000	-1.486500000
6	-4.001208000	1.174604000	-1.113629000
1	-4.423058000	1.492535000	-2.092286000
1	-4.825634000	1.276938000	-0.368237000
6	-3.537505000	-0.283682000	-1.184620000
1	-4.382958000	-0.939375000	-1.485258000
1	-2.763511000	-0.368793000	-1.975096000
6	-2.941757000	-0.787970000	0.144638000
1	-3.726764000	-0.664192000	0.929693000
6	1.854181000	0.076081000	-0.066585000
6	2.580728000	-1.095126000	-0.398680000
6	3.929333000	-0.951828000	-0.785383000
1	4.512935000	-1.849622000	-1.042194000
6	4.528566000	0.310695000	-0.871502000
1	5.586504000	0.401571000	-1.164049000
6	3.765841000	1.461519000	-0.627063000
1	4.223851000	2.453664000	-0.756753000
6	2.416130000	1.371131000	-0.235008000
6	0.980276000	-1.431123000	2.510062000
1	2.075822000	-1.407569000	2.339919000
1	0.568114000	-2.340269000	2.030554000
1	0.808255000	-1.515348000	3.602830000
6	0.878423000	1.060468000	2.718791000
1	1.956708000	1.193759000	2.496669000
1	0.772944000	0.914235000	3.813266000
1	0.346589000	1.993958000	2.452409000

6	-3.278011000	3.568911000	-0.609276000
1	-4.058066000	3.703930000	0.172184000
1	-3.700604000	3.932509000	-1.569375000
1	-2.423131000	4.227177000	-0.345420000
6	-2.591980000	-2.303453000	0.095589000
1	-1.934079000	-2.514785000	0.968592000
6	-1.807271000	-2.702994000	-1.163526000
1	-2.460519000	-2.726634000	-2.060815000
1	-1.362817000	-3.713665000	-1.050293000
1	-0.993436000	-1.974865000	-1.367114000
6	-3.845936000	-3.175496000	0.270771000
1	-3.588305000	-4.255438000	0.257340000
1	-4.575462000	-3.002363000	-0.549336000
1	-4.362681000	-2.960962000	1.229987000
6	1.906744000	-2.457971000	-0.512170000
1	0.911495000	-2.384186000	-0.032616000
6	1.661145000	-2.761045000	-2.005784000
1	1.101473000	-3.711455000	-2.129444000
1	2.622455000	-2.852915000	-2.554228000
1	1.075394000	-1.947479000	-2.478613000
6	2.685661000	-3.594861000	0.168952000
1	2.877940000	-3.379183000	1.239417000
1	3.666954000	-3.771817000	-0.319483000
1	2.115323000	-4.545042000	0.107725000
6	1.554771000	2.626895000	-0.149260000
1	0.688271000	2.397738000	0.498289000
6	2.275795000	3.839709000	0.456621000
1	1.566316000	4.683652000	0.582597000
1	3.098237000	4.204843000	-0.193883000
1	2.709739000	3.604520000	1.450576000
6	0.980492000	2.932635000	-1.549280000
1	1.794609000	3.152901000	-2.271928000
1	0.302059000	3.811354000	-1.512101000
1	0.405890000	2.057774000	-1.917807000

TS2

7	0.555128000	-0.151843000	0.427493000
6	-0.513111000	0.057392000	-0.357455000
6	-1.759556000	0.152221000	0.510865000
6	-1.293593000	-0.444611000	1.871220000
1	-1.738927000	0.088062000	2.735532000
1	-1.602172000	-1.503455000	1.942226000
6	0.255304000	-0.380213000	1.896478000
6	-2.061451000	1.676642000	0.669368000

1	-2.905653000	1.782070000	1.389825000
1	-1.191628000	2.187993000	1.133904000
6	-2.419881000	2.367201000	-0.654067000
1	-1.542343000	2.245372000	-1.328067000
6	-3.609521000	1.645763000	-1.305759000
1	-3.822189000	2.088044000	-2.303626000
1	-4.517622000	1.828850000	-0.683598000
6	-3.386035000	0.132656000	-1.432286000
1	-4.299262000	-0.334242000	-1.852882000
1	-2.570289000	-0.082393000	-2.157531000
6	-3.046282000	-0.516922000	-0.076036000
1	-3.860440000	-0.201463000	0.619621000
6	1.904002000	-0.040501000	-0.067676000
6	2.612608000	-1.209774000	-0.454684000
6	3.966505000	-1.072809000	-0.825350000
1	4.534630000	-1.969126000	-1.119823000
6	4.589992000	0.180340000	-0.853092000
1	5.650343000	0.264052000	-1.139121000
6	3.848830000	1.332660000	-0.557066000
1	4.326570000	2.321550000	-0.635742000
6	2.496302000	1.249524000	-0.174002000
6	0.870030000	-1.690502000	2.404574000
1	1.975745000	-1.672692000	2.325027000
1	0.486861000	-2.562629000	1.841363000
1	0.608910000	-1.832090000	3.473443000
6	1.933597000	-2.568237000	-0.607073000
1	0.896273000	-2.472112000	-0.224319000
6	1.810874000	-2.923664000	-2.104166000
1	1.274816000	-3.887973000	-2.226632000
1	2.810052000	-3.021238000	-2.580112000
1	1.230780000	-2.149756000	-2.644197000
6	2.654525000	-3.693685000	0.156938000
1	2.783789000	-3.455405000	1.231253000
1	3.662957000	-3.888750000	-0.265309000
1	2.080712000	-4.640740000	0.081935000
6	1.680608000	2.526047000	-0.004392000
1	0.729347000	2.250381000	0.486565000
6	2.369937000	3.585565000	0.870200000
1	1.696574000	4.453774000	1.027741000
1	3.296985000	3.974047000	0.398601000
1	2.643663000	3.178892000	1.865072000
6	1.313947000	3.087607000	-1.394018000
1	2.222916000	3.391599000	-1.955239000
1	0.655306000	3.976346000	-1.298195000

1	0.780378000	2.323367000	-1.994159000
1	-0.538133000	-0.421160000	-1.450403000
1	-0.805386000	-1.524296000	-1.611873000
6	-3.036118000	-2.086085000	-0.054529000
6	-3.479433000	-2.756589000	-1.363446000
6	-3.884793000	-2.617437000	1.115088000
1	-1.979558000	-2.402801000	0.095649000
1	-2.821104000	-2.458290000	-2.203701000
1	-3.415159000	-3.860638000	-1.263270000
1	-4.530407000	-2.511467000	-1.626478000
1	-3.580641000	-2.182795000	2.090306000
1	-4.957582000	-2.364075000	0.966719000
1	-3.812481000	-3.722413000	1.200622000
6	-2.677882000	3.864422000	-0.458020000
1	-2.912283000	4.364108000	-1.421280000
1	-3.537290000	4.037153000	0.226330000
1	-1.793930000	4.373976000	-0.018832000
6	0.804280000	0.782643000	2.743176000
1	0.614107000	0.581439000	3.816592000
1	1.899529000	0.888776000	2.605194000
1	0.325234000	1.747117000	2.489677000

CAAC-H_2

7	0.600207000	-0.048311000	0.480516000
6	-0.562942000	-0.219667000	-0.372198000
6	-1.743999000	0.246010000	0.508876000
6	-1.276861000	-0.221255000	1.913448000
1	-1.697985000	0.422191000	2.712903000
1	-1.633044000	-1.251409000	2.114450000
6	0.283179000	-0.209816000	1.925768000
6	-1.844879000	1.793322000	0.508088000
1	-2.527257000	2.097249000	1.335351000
1	-0.850326000	2.218867000	0.753933000
6	-2.362513000	2.414249000	-0.796887000
1	-1.652981000	2.142255000	-1.613545000
6	-3.726838000	1.800443000	-1.144323000
1	-4.102495000	2.209429000	-2.107842000
1	-4.465007000	2.103238000	-0.364973000
6	-3.646027000	0.271684000	-1.209570000
1	-4.645186000	-0.151479000	-1.450070000
1	-2.980231000	-0.015841000	-2.052834000
6	-3.123983000	-0.356685000	0.098964000
1	-3.819420000	-0.020678000	0.904128000
6	1.919949000	-0.140138000	-0.052074000

6	2.477203000	-1.388682000	-0.464691000
6	3.799826000	-1.423958000	-0.950920000
1	4.234126000	-2.386720000	-1.264792000
6	4.569446000	-0.257846000	-1.048928000
1	5.605658000	-0.307541000	-1.419713000
6	4.002310000	0.975275000	-0.702101000
1	4.591422000	1.898163000	-0.825557000
6	2.680778000	1.057641000	-0.221858000
6	0.830167000	-1.522547000	2.530064000
1	1.933702000	-1.574726000	2.425947000
1	0.392440000	-2.413998000	2.039522000
1	0.587304000	-1.581412000	3.611541000
6	1.652056000	-2.672433000	-0.483390000
1	0.718168000	-2.469117000	0.073442000
6	1.255189000	-3.027491000	-1.931784000
1	0.588294000	-3.915239000	-1.954401000
1	2.151488000	-3.257940000	-2.546046000
1	0.724908000	-2.185327000	-2.421260000
6	2.355052000	-3.855762000	0.203757000
1	2.646870000	-3.606062000	1.243658000
1	3.274106000	-4.160921000	-0.339305000
1	1.685415000	-4.740735000	0.237575000
6	2.042833000	2.425126000	-0.011265000
1	1.093236000	2.240321000	0.524347000
6	2.898648000	3.382873000	0.831534000
1	2.350138000	4.328692000	1.024767000
1	3.846406000	3.653925000	0.319222000
1	3.163401000	2.935272000	1.811192000
6	1.675995000	3.047882000	-1.374133000
1	2.582372000	3.241767000	-1.986765000
1	1.142510000	4.012756000	-1.238535000
1	1.017433000	2.371648000	-1.956743000
1	-0.453171000	0.384614000	-1.299274000
1	-0.724463000	-1.275048000	-0.702507000
6	-3.199434000	-1.920782000	0.080939000
6	-3.012973000	-2.577435000	-1.299943000
6	-4.521501000	-2.395470000	0.708580000
1	-2.378017000	-2.303011000	0.726998000
1	-2.078309000	-2.257462000	-1.802653000
1	-2.968624000	-3.681462000	-1.192564000
1	-3.856793000	-2.349381000	-1.983638000
1	-4.621199000	-2.045097000	1.757143000
1	-5.393472000	-2.003006000	0.140843000
1	-4.599199000	-3.503177000	0.710283000

6	-2.410383000	3.943447000	-0.708356000
1	-2.764174000	4.395322000	-1.658706000
1	-3.101555000	4.272605000	0.097913000
1	-1.408593000	4.365717000	-0.483038000
6	0.853160000	0.956927000	2.761219000
1	0.639987000	0.802729000	3.839082000
1	1.954133000	1.019608000	2.640733000
1	0.415801000	1.929122000	2.463283000

A (singlet)

45	0.000002000	0.409309000	-0.000887000
15	-1.162394000	-1.280136000	-1.027841000
15	1.164102000	-1.277633000	1.027921000
7	-2.768321000	-1.745039000	-0.815409000
7	1.209367000	-1.456291000	2.705503000
7	2.770208000	-1.742345000	0.816169000
7	-1.207687000	-1.460630000	-2.705247000
7	-2.134725000	2.478560000	-0.962972000
7	2.133952000	2.481190000	0.957073000
6	-1.284387000	1.730130000	-0.619451000
6	1.283598000	1.731949000	0.615365000
6	3.299111000	-2.275053000	-0.404202000
6	0.001224000	-1.937971000	0.000339000
6	3.349606000	-3.684259000	-0.560317000
6	2.752394000	-4.592508000	0.486524000
1	3.345121000	-4.599697000	1.426686000
1	2.701579000	-5.637284000	0.124320000
1	1.724838000	-4.269912000	0.757004000
6	-0.040730000	-1.360897000	-3.535404000
6	4.472541000	-3.373059000	-2.726066000
6	0.777452000	-2.504260000	-3.721903000
6	-3.297501000	-2.275309000	0.405915000
6	3.760800000	-1.408744000	-1.423553000
6	4.352181000	-1.980678000	-2.564927000
1	4.725973000	-1.312220000	-3.356643000
6	-3.228800000	3.259915000	-1.445066000
6	-3.346314000	-3.684163000	0.565467000
6	0.042594000	-1.352984000	3.535357000
6	-3.939443000	-4.206457000	1.728275000
1	-3.985143000	-5.300684000	1.856871000
6	-2.467012000	-2.047286000	-3.190034000
1	-2.357916000	-3.143216000	-3.361634000
1	-2.754875000	-1.577287000	-4.152338000
6	5.152045000	-3.960981000	-3.939424000

1	5.195879000	-3.236226000	-4.775782000
1	4.634105000	-4.874748000	-4.296688000
1	6.197640000	-4.256636000	-3.704066000
6	0.510153000	-3.782360000	-2.966360000
1	-0.495875000	-4.200453000	-3.181405000
1	0.568066000	-3.600002000	-1.871406000
1	1.261355000	-4.554113000	-3.218499000
6	2.468555000	-2.042438000	3.191122000
1	2.359596000	-3.138234000	3.363611000
1	2.756144000	-1.571495000	4.153042000
6	2.176745000	-1.208428000	-5.276790000
6	1.369243000	-0.080645000	-5.035686000
1	1.601636000	0.868726000	-5.546248000
6	3.942494000	-4.208650000	-1.722303000
1	3.989511000	-5.303130000	-1.848245000
6	-3.506246000	-1.756335000	-2.087817000
1	-4.003331000	-0.774629000	-2.264060000
1	-4.295606000	-2.533030000	-2.053166000
6	1.863193000	-2.408012000	-4.608824000
1	2.485898000	-3.299478000	-4.778191000
6	0.253826000	-0.133638000	-4.177922000
6	3.507895000	-1.752292000	2.088765000
1	4.004660000	-0.770268000	2.264117000
1	4.297485000	-2.528772000	2.054971000
6	-0.776792000	-2.495191000	3.724484000
6	3.367124000	-1.124768000	-6.201973000
1	3.610514000	-2.110799000	-6.645139000
1	4.272440000	-0.777365000	-5.656204000
1	3.194977000	-0.406741000	-7.028617000
6	-0.509333000	-3.775790000	2.973247000
1	0.494970000	-4.195392000	3.193483000
1	-0.562593000	-3.596373000	1.877587000
1	-1.263128000	-4.545283000	3.224537000
6	-2.746985000	-4.594026000	-0.478738000
1	-3.336655000	-4.601060000	-1.420793000
1	-2.698578000	-5.638580000	-0.115579000
1	-1.718142000	-4.272874000	-0.746111000
6	-4.471400000	-3.369058000	2.729528000
6	-3.761364000	-1.407059000	1.422592000
6	3.228033000	3.263569000	1.437544000
6	-4.202887000	2.333171000	-2.220716000
1	-4.555672000	1.529142000	-1.539475000
1	-3.652768000	1.849378000	-3.055930000
6	3.578089000	0.081127000	-1.313484000

1	4.207778000	0.622208000	-2.045640000
1	3.811988000	0.448549000	-0.294709000
1	2.515612000	0.355058000	-1.507398000
6	-1.863176000	-2.395529000	4.610087000
1	-2.486786000	-3.285975000	4.781447000
6	-3.580354000	0.082749000	1.308977000
1	-2.518472000	0.358333000	1.503743000
1	-4.211780000	0.624914000	2.038838000
1	-3.813185000	0.447329000	0.288950000
6	-4.638797000	5.839374000	-1.733661000
1	-5.484461000	6.456670000	-2.104550000
1	-3.957593000	6.524213000	-1.183407000
6	-5.150899000	-3.954768000	3.943948000
1	-6.196432000	-4.251076000	3.709129000
1	-5.194952000	-3.228382000	4.778895000
1	-4.632823000	-4.867725000	4.303055000
6	-0.251273000	-0.123779000	4.174305000
6	-4.352919000	-1.976917000	2.564918000
1	-4.728351000	-1.306972000	3.354612000
6	-2.704396000	4.366155000	-2.397051000
1	-2.150237000	3.890776000	-3.234071000
1	-1.987680000	5.010602000	-1.845193000
6	-4.862011000	4.265475000	-3.694386000
1	-4.342215000	3.807643000	-4.564064000
1	-5.711330000	4.854787000	-4.100579000
6	-0.582716000	1.097080000	-3.934431000
1	-0.208299000	1.645284000	-3.043579000
1	-1.638370000	0.839853000	-3.720225000
1	-0.547500000	1.787204000	-4.800014000
6	-1.367431000	-0.067469000	5.031047000
1	-1.599336000	0.883459000	5.538927000
6	-5.389167000	3.165095000	-2.748460000
1	-6.078609000	2.491948000	-3.301003000
6	-2.176248000	-1.193700000	5.274423000
6	-3.977336000	3.910379000	-0.252594000
1	-3.269580000	4.551503000	0.314444000
1	-4.327351000	3.111239000	0.434548000
6	-6.130422000	3.810855000	-1.557925000
1	-6.528627000	3.023761000	-0.881142000
1	-7.003126000	4.391716000	-1.924857000
6	-5.164460000	4.737535000	-0.788505000
1	-5.693196000	5.200348000	0.071420000
6	-3.897133000	5.191724000	-2.923076000
1	-3.511836000	5.981824000	-3.601662000

6	2.703869000	4.370029000	2.389398000
1	2.150896000	3.894801000	3.227280000
1	1.986183000	5.013699000	1.837891000
6	0.586532000	1.105765000	3.929093000
1	1.638365000	0.846089000	3.700092000
1	0.564299000	1.790027000	4.799808000
1	0.203165000	1.661708000	3.046895000
6	-3.367589000	-1.106590000	6.198055000
1	-4.273803000	-0.767411000	5.648609000
1	-3.198801000	-0.380970000	7.018699000
1	-3.607677000	-2.089775000	6.649330000
6	3.896595000	5.196701000	2.913733000
1	3.511436000	5.986926000	3.592252000
6	3.974921000	3.913814000	0.243935000
1	3.266153000	4.554108000	-0.322777000
1	4.324776000	3.114501000	-0.443093000
6	4.862888000	4.271559000	3.684589000
1	4.344289000	3.813890000	4.555066000
1	5.712214000	4.861708000	4.089551000
6	4.636589000	5.844154000	1.723189000
1	5.482223000	6.462254000	2.092817000
1	3.954361000	6.528212000	1.173228000
6	4.203541000	2.337942000	2.212775000
1	3.654631000	1.854384000	3.048916000
1	4.556108000	1.533677000	1.531701000
6	5.162030000	4.742109000	0.778144000
1	5.689564000	5.204766000	-0.082595000
6	5.389812000	3.170971000	2.738774000
1	6.080275000	2.498612000	3.291012000
6	6.129419000	3.816527000	1.547112000
1	6.527453000	3.029309000	0.870373000
1	7.002105000	4.398187000	1.912825000

IX. References

1. Hu, C., Wang, X.-F., Li, J., Chang, X.-Y. & Liu, L. L. A stable rhodium-coordinated carbene with a $\sigma^0\pi^2$ electronic configuration. *Science* **383**, 81–85 (2024).
2. Sivak, A. & Muetterties, E. L. Metal clusters. 21. Synthesis of rhodium phosphite clusters. *J. Am. Chem. Soc.* **101**, 4878–4887 (1979).
3. Frisch, M. J. et al. Gaussian 16 rev. B.01 (Gaussian, Inc., Wallingford, CT, 2016).
4. Lee, C., Yang, W. & Parr, R. G. Development of the colle-salvetti correlation-energy formula into a functional of the electron density. *Phys. Rev. B* **37**, 785–789 (1988).
5. Stephens, P. J., Devlin, F. J., Chabalowski, C. F. & Frisch, M. J. Ab initio calculation of vibrational absorption and circular dichroism spectra using density functional force fields. *J. Phys. Chem.* **98**, 11623–11627 (1994).
6. Grimme, S., Antony, J., Ehrlich, S. & Krieg, H. A consistent and accurate ab initio parametrization of density functional dispersion correction (DFT-D) for the 94 elements H-Pu. *J. Chem. Phys.* **132**, 154104–154133 (2010).
7. Grimme, S. Semiempirical GGA-type density functional constructed with a long-range dispersion correction. *J. Comput. Chem.* **27**, 1787–1799 (2006).
8. Grimme, S. Accurate description of van der Waals complexes by density functional theory including empirical corrections. *J. Comput. Chem.* **25**, 1463–1473 (2004).
9. Deng, L., Ziegler, T. & Fan, L. A combined density functional and intrinsic reaction coordinate study on the ground state energy surface of H_2CO. *J. Chem. Phys.* **99**, 3823–3835 (1993).
10. Deng, L. & Ziegler, T. The determination of intrinsic reaction coordinates by density functional theory. *Int. J. Quantum Chem.* **52**, 731–765 (1994).
11. Glendening, E. D., Badenhoop, J. K., Reed, A. E., Carpenter, J. E., Bohmann, J. A., Morales, K. P. C. M., Landis, C. R. & Weinhold, F. NBO 7.0 (Univ. of Wisconsin, Madison, WI, 2018).
12. Neese, F. The ORCA program system. Wiley Interdiscip. *Rev. Comput. Mol. Sci.* **2**, 73–78 (2012).
13. Legault, C. Y. CYLview, 1.0b (Univ. de Sherbrooke, Sherbrooke, Quebec, Canada, 2009); https://www.cylview.org.
14. Andrienko, G. A. ChemCraft (2024); http://www.chemcraftprog.com.
15. Knizia, G. & Klein, J. E. M. N. Electron flow in reaction mechanisms—revealed from first principles. *Angew. Chem. Int. Ed.* **54**, 5518–5522 (2015).
16. O'Boyle, N. M., Tenderholt, A. L. & Langner, K. M. Cclib: A Library for package-independent computational chemistry algorithms. *J. Comput. Chem.* **29**, 839–845 (2008).
17. Marenich, A.V., Cramer, C.J. & Truhlar, D.G. Universal solvation model based on solute electron density and on a continuum model of the solvent defined by the bulk dielectric constant and atomic surface tensions. *J. Phys. Chem. B* **113**, 6378–6396 (2009).
18. Savin, A., Nesper, R., Wengert, S. & Fässler, T. F. ELF: the electron localization function. *Angew. Chem. Int. Ed. Engl.* **36**, 1808–1832 (1997).
19. van Gisbergen, S., Snijders, J. & Ziegler, T. Chemistry with ADF. *J. Comput. Chem.* **22**, 931–967 (2001).
20. Grimme, S. Exploration of chemical compound, conformer, and reaction space with meta-dynamics simulations based on tight-binding quantum chemical calculations. *J. Chem. Theory Comput.* **15**, 2847–2862 (2019).

21. Chai, J. D. & Head-Gordon, M. Systematic optimization of long-range corrected hybrid density functionals. *J. Chem. Phys.* **128**, 084106 (2008).
22. Klamt, A. & Schüürmann, G. COSMO: A new approach to dielectric screening in solvents with explicit expressions for the screening energy and its gradient. *J. Chem. Soc., Perkin Trans.* **2**, 799–805 (1993).
23. Andzelm, J., Kölmel, C. & Klamt, A. Incorporation of solvent effects into density functional calculations of molecular energies and geometries. *J. Chem. Phys.* **103**, 9312–9320 (1995).
24. Barone, V. & Cossi, M. Quantum calculation of molecular energies and energy gradients in solution by a conductor solvent model. *J. Phys. Chem. A* **102**, 1995–2001 (1998).
25. Cossi, M., Rega, N., Scalmani, G. & Barone, V. Energies, structures, and electronic properties of molecules in solution with the C-PCM solvation model. *J. Comput. Chem.* **24**, 669–681 (2003).
26. Hanwell, M.D., Curtis, D.E., Lonie, D.C., Vandermeersch, T., Zurek, E. & Hutchison, G.R. Avogadro: an advanced semantic chemical editor, visualization, and analysis platform. *J. Cheminform.* **4**, 17 (2012).